理學博士學位論文

Abelson interacting protein (Abi) Regulation of Notch-Mediated Hematopoiesis

조혈과정에서 Abelson 상호작용 단백질인 Abi에 의한 Notch 신호전달의 조절

2019년 8월

서울대학교 대학원
협동과정 뇌과학전공

박 선 영

Abstract

Abelson interacting protein (Abi) Regulation of Notch-Mediated Hematopoiesis

Sun-Young Park

Interdisciplinary Graduate Program in Neuroscience

The Graduate School

Seoul National University

Abelson interacting protein (Abi) is a component of the SCAR complex and transmits small GTPase Rac1 signaling to the Arp2/3 complex, triggering actin assembly. Previous reports have demonstrated that Abi and SCAR are critical for Rac-dependent membrane protrusion and macropinocytosis. In addition, Abi regulates actin polymerization through the signaling cascade involving another small GTPase molecule, Cdc42, and its downstream effector, the WASp protein. However, it has not been elucidated the biological significance of actin regulation of Abi via Cdc42-WASp. Here, I investigated the Abi influences on hematopoiesis in *Drosophila*. Expression data demonstrated that Abi

acts cell-autonomously in hematopoiesis. Loss of Abi led to a substantial decrement in the crystal cell population and downregulation of Notch response element in the late third instar larval stage. Genetic studies revealed that *abi* and *notch* interact to participate in the differentiation process of crystal cells. These results implicate that Abi is essential for transdifferentiation to crystal cells via positive modulation of Notch signaling. For controlling of Notch signaling, Abi promotes clathrin-dependent endocytosis of Notch receptor by actin regulation through Cdc42-WASp pathway rather than Rac1-SCAR pathway. My research on identifying the physiological function of *Drosophila* Abi in hematopoiesis will serve as fundamental data for the pathophysiological study of myeloproliferative neoplasms exhibiting the loss of human Abi.

Keywords: Abi, Notch signaling, Crystal cell, Transdifferentiation, Endocytosis, Hematopoiesis

Student Number: 2010-30122

Table of Contents

List of Figures

Abbreviations

Abi	Abelson interacting protein, Abl interactor
Abl	Abelson
ADP	Adenosine diphosphate
AEL	After egg laying
AML	Acute myeloid leukemia
Arp2/3	Actin related protein 2/3
AP	Adaptor protein
BCR	Breakpoint cluster region
BMP	Bone morphogenetic protein
BSA	Bovine serum albumin
bp	Base pair
CDE	Clathrin-dependent endocytosis
Chc	Clathrin heavy chain
CIE	Clathrin-independent endocytosis
CML	Chronic myeloid leukemia
CtBP1	C-terminal binding protein-1
Cy	Cyanine fluorescent dye
CYFIP	Cytoplasmic Fragile X mental retardation1-interacting protein
DAPI	4,6-diamidino-2-phenylindole
Df	Deficiency
DNA	Deoxyribonucleic acid
DSL	Delta/Serrate/Lag-2
dsRed	Discosoma Red fluorescent protein

dsRNA	Double strand ribonucleic acid
EGFP	Enhanced green fluorescent protein
EGFR	Epidermal growth factor receptor
ET	Essential thrombocythemia
F-actin	Filamentous actin
FITC	Fluorescein isothiocyanate
FBS	Fetal bovine serum
Gbb	Glass bottom boat
GEEC	GPI-enriched endocytic compartment
GFP	Green fluorescent protein
GPI	Glycosylphosphatidylinositol
Graf	GTPase regulator associated with focal adhesion kinase
GTP	Guanosine-5'-triphosphate
HHR	Homeodomain homologous region
Hml	Hemolectin
HSC	Hematopoietic stem cell
HSPC300	Haematopoietic stem/progenitor cell protein 300
JAK	Janus kinase
Lz	Lozenge
MLL	Myeloid/lymphoid or mixed-lineage leukemia
MPNs	Myeloproliferative neoplasms
Mt	Metallothionein
N	Notch
Nap	Nck-associated protein
Necd	Extracellular domain of Notch

Nicd	Intracellular domain of Notch
NimC1	Nimrod C1
NESH	New molecule including SH3
NK cell	Natural Killer cell
NRE	Notch response element
PBS	Phosphate buffered saline
PCR	Polymerase chain reaction
PLL	Poly-L-lysine
PMF	Primary myelofibrosis
PO	Phenoloxidase
PP	Polyproline
PPO	Prophenoloxidase
PRR	Proline-rich region
PV	Polycythemia vera
Pvr	PDGF-/VEGF-receptor related
Rab	Ras-related proteins in brain
RNAi	RNA interference
rpm	Revolutions per minute
rp49	Ribosomal protein 49
RT-PCR	Reverse transcription polymerase chain reaction
RUNX	Runt-related transcription factor
Sara	Smad anchor for receptor activation
SCAR	Suppressor of cAMP receptor
SEM	Standard error of the mean
Ser	Serrate
SH3	Src homology 3

SR	Serine/threonine-rich region
Sra	Steroid receptor RNA activator
Srp	Serpent
STAT	Signal transducer and activator of transcription
TfR	transferrin receptor
Twf	Twinfilin
UAS	Upstream activating sequence
WAB	WAVE-binding
WASP,WASp	Wiskott-Aldrich syndrome protein
WAVE	WASP-family verprolin homology protein
WT	Wild-type

Introduction

1. *Drosophila melanogaster* as a model system of hematopoietic development

Hematopoiesis is the process of forming the blood cells that compose the immune system. These immune cells are responsible for the immune response within individual organisms and maintain the homeostasis that plays a vital role in survival. The hematopoietic stem cells (HSCs) differentiate progenitor cells, which include myeloid progenitor cells and lymphoid progenitor cells. The lymphoid progenitor cells are differentiated into cell lines associated with the adaptive immune system such as B cells, T cells, and Natural Killer cells (NK cells). The myeloid progenitor cells introduced previously are differentiated into erythrocytes, granulocytes, macrophages, mast cells, megakaryocytes and so forth. This myelopoiesis proceeds in the bone marrow of vertebrates and regulates innate immunity or blood coagulation. Thus, studying hematopoiesis provides a better understanding of disorders that are linked to the dysregulation of this process.

Myeloproliferative neoplasms (MPNs) are a group of clonal diseases characterized by the hyperproliferation of myeloid cells in the bone marrow (Dameshek, 1951; Vardiman et al., 2009). One in particular, chronic myeloid leukemia (CML), results from an abnormal hyperplastic state of hematopoietic stem cells in the bone marrow (Quintas-Cardama and Cortes, 2009). The MPNs are related to acute myeloid leukemia (AML) which is a malignancy of

immature cells in the bone marrow (Döhner et al., 2015). Primary myelofibrosis (PMF) is a chronic MPN characterized by bone marrow fibrosis (Barbui et al., 2018). Because of the fibrosis, the hematopoietic stem cells are unable to produce enough normal blood cells. The reduction in the number of blood cells causes anemia with nucleated and teardrop-shaped red blood cells and splenomegaly.

The immune cells of invertebrates are called hemocytes, and the *Drosophila* hemocytes are differentiated from prohemocytes, as precursors, to three types of circulating hemocytes (Figure 1). The process of hemocyte production in flies formed through two streams, embryonic hematopoiesis for larval stages and larval hematopoiesis for adult stages (Meister, 2004; Milchanowski et al., 2004; Evans et al., 2008). Plasmatocytes are the most abundant cells of *Drosophila* hemocytes having high rates of self-renewal. They have a phagocytic activity to dead cells and bacteria like vertebrate macrophage. The second type of hemocytes is the crystal cell, named for its crystal structured cytoplasm. Crystal cells are vertebrate platelet-like cells that have functions in wound healing and clotting against cuticle injury and microbial invasion (Rizki et al., 1980; Gajewski et al., 2007). Mature crystal cells can release prophenol oxidase required for melanization, where soft clots are formed by coagulation of hemolymph and hardened via localized melanization at wound sites. The third type of *Drosophila* hemocytes is lamellocyte, which is a large, flat, and adherent cell rarely founded under normal conditions. Lamellocytes are

Figure 1. Differentiation of hemocytes in *Drosophila*.

Prohemocytes as multipotent progenitors differentiate three types of hemocytes. Plasmatocytes constitute around 95% of the hemocyte population. The major function of plasmatocytes is phagocytosis of apoptotic cells and invading bacteria. Crystal cells include enzymatic crystalline in the cytoplasm. Disruption of crystal cells promotes enzymatic activity for melanization that is necessary for wound healing and clotting. Lamellocytes are rarely founded under healthy conditions and differentiated in response to infestation, resulting in encapsulation of parasite wasp egg.

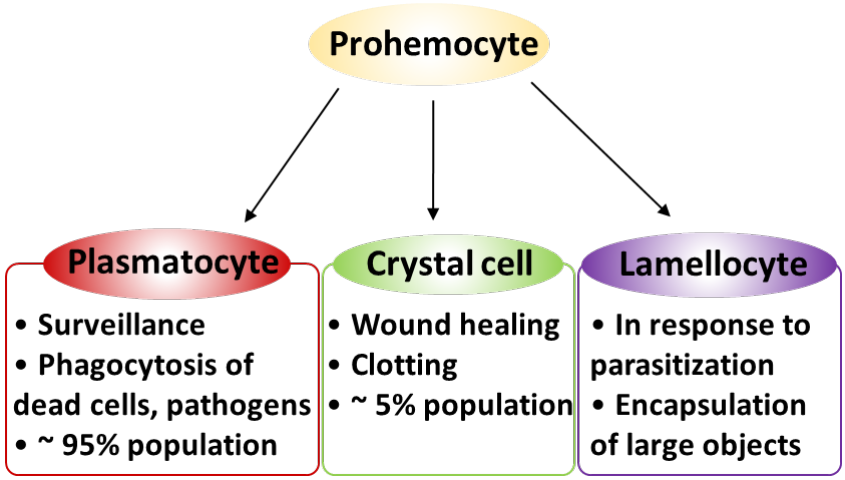
Prohemocyte
Plasmatocyte
• Surveillance
• Phagocytosis of dead cells, pathogens
• ~ 95% population
Crystal cell
• Wound healing
• Clotting
• ~ 5% population
Lamellocyte
• In response to parasitization
• Encapsulation of large objects

differentiated in response to parasitization by wasps such as *Leptopilina boulardi* or in metamorphosis having encapsulation activity (Rizki TM and Rizki RM, 1992).

During hematopoiesis, differentiation from progenitor cells should be tightly regulated by signal transduction pathways. The signal transduction pathways that contributed to the production and differentiation of hemocytes are very similar to that of mammalians, and the transcription factors involved in *Drosophila* hematopoiesis are evolutionarily preserved (Waltzer et al., 2003). The GATA family of transcriptional factors is conserved between humans and fruit flies and these factors mediate developmental programs of blood cells (Orkin et al., 1998; Cantor and Orkin, 2002; Maduro and Rothman, 2002). In *Drosophila*, Serpent (Srp) has fundamental roles in promoting hematopoietic development in embryonic head mesoderm, corresponding to murine GATA family (Shivdasani et al., 1997; Pai et al., 2003; Rodrigues et al., 2005). With Srp, Lozenge (Lz) works together to determine the crystal cell fate and to control the crystal cell differentiation, serving as a representative marker of crystal cells. Fly Lz shows high similarity to human Runx1 transcription factors (Daga et al., 1996).

One of the well-conserved signaling pathways in *Drosophila* hematopoiesis is Notch signaling. The signal transduction pathway mediated by Notch receptor controls development and homeostasis. The Notch is a heterodimer composed of the extracellular domain (Necd) and the intracellular domain (Nicd), held together noncovalently. The ligands of Notch belong to Delta/Serrate/Lag-2

(DSL) family which are also transmembrane proteins. There are one Notch receptor and two ligands of Notch, Delta and Serrate, in *Drosophila*. Notch signaling takes place between juxtaposed neighboring cells due to the nature of ligand and receptor and is initiated by the binding of a ligand to Notch. The ligand-activated Notch is internalized to Rab5-positive early endosomes or Sara-positive signaling endosomes (Loubéry et al., 2014; Montagne and Gonzalez-Gaitan 2014; Chapman et al., 2016). After cleavage by γ-secretase, the intracellular domain of Notch is released and translocated into the nucleus then functions as a transcriptional coactivator.

Notch signaling is generally known to act in the crystal cell development during *Drosophila* hematopoiesis. Lz is considered to be a part of the downstream of Notch and in combination with Notch at target enhancers, *klumpfuss* and *pebbled/hindsight* (Terriente-Felix et al., 2013). Circulating crystal cell population is formed through two differentiation processes until late third instar larval stage. Embryonic Lz is expressed in crystal cell precursors located in head mesoderm at stage 7 (Bataillé et al., 2005). Sessile hemocyte clusters are the hematopoietic tissues that provide the cell fate transition from plasmatocyte into the crystal cell during larval stages (Markus et al., 2009; Leitão and Sucena, 2015). Serrate-Notch signaling participates plasmatocyte transdifferentiation in sessile clusters. Expression of a general Notch reporter, Notch response element (NRE)-EGFP, indicates that Notch activation is specific on Lz-expressing crystal cells. These reports

demonstrate that Notch signaling is essential for the formation of the crystal cell population, but it was not clear how Notch signaling could be regulated and transmitted during the crystal cell development.

2. The characteristics of Abi proteins and their roles in hematopoiesis

Actin polymerization is regulated by members of the Rho family of small GTPases (Hall, 1998; Begum et al., 2004). Specifically, Rac and Cdc42 are activated in response to extracellular signals and triggers actin-related protein 2/3 (Arp2/3) complex (Soderling, 2009; Kurisu and Takenawa, 2009; Jia et al., 2010). The Arp2/3 complex activates filamentous actin (F-actin) nucleation. One of the Arp2/3 activators is Wiskott-Aldrich syndrome protein (WASP, WASp) initially identified in patients with Wiskott-Aldrich syndrome, an X chromosome-linked disease characterized by immune disorders and thrombocytopenia (Parolini et al., 1997). Another regulator of Arp2/3-dependent actin nucleation is WASP family verprolin homologous (WAVE) protein, also known as suppressor of cAMP receptor (SCAR) protein in *Drosophila*. WASP and WAVE proteins are maintained in an inactive state in the cytosol under resting conditions. In response to extracellular stimuli, autoinhibitions of WASP and WAVE are relieved by the binding of GTP-bound Cdc42 and Rac1, respectively.

Abelson interacting protein or Abl interactor, commonly known as Abi, was originally identified as a substrate adaptor protein for

the Abl tyrosine kinase protein (Tani et al., 2003). A generally known feature of Abi is a multi-modular protein that interacts with several key regulators of actin dynamics (Figure 2). It consists of an amino-terminal WAVE-binding (WAB) domain, a homeodomain homologous region (HHR), three of proline-rich regions (PRRs), and a carboxyl-terminal SH3 domain. Abi protein directly binds to SCAR/WAVE protein through its N-terminal WAB domain (Echarri et al., 2004) while also binding to Kette/NAP1 via central HHR (Bogdan et al., 2004) and interacting with WASp protein through the C-terminal Src homology 3 (SH3) domain (Bogdan et al., 2005). Abi protein is a crucial component of the SCAR/WAVE complex, which relays signals from Rac1 to Arp2/3. Abi, Kette, and Sra1 control the stability of SCAR/WAVE complex to regulate the formation of actin protrusions (Kunda et al., 2003). It has been identified that there are three Abi family proteins found in vertebrates (Figure 3). Abi1 and Abi2 were initially identified as proteins that bind to the PxxP motif in Abl and negatively modulated its transforming activity (Shi et al., 1995; Dai and Pendergast, 1995). A third member, Abi3, was identified as a novel gene in humans (NESH) that possesses an SH3 domain and was later incorporated into the Abi family based on amino acid sequence similarity (Miyazaki et al., 2000). However, its binding activity with Abl has not been identified (Hirao et al., 2006; Sato M et al., 2012). In *Drosophila*, there is one Abi protein corresponding to vertebrate proteins with high similarity.

Actin regulation is accompanied by changing the shape of the

Figure 2. Domain structure of Abi and its interacting proteins.

The schematic of the domain structure of *Drosophila* Abi. It contains a WAVE-binding (WAB) domain, a homeodomain homologous region (HHR), three of proline-rich regions (PRRs), and a Src homology 3 (SH3) domain. The black boxes represent the proline-rich region. P in the round means phosphorylation site by Abl kinase. The interacting protein of the individual domain indicates a double-sided arrow. N-terminal WAB and HHR domains respectively interact with SCAR/WAVE and kette/Nap1 which are WAVE complex components stimulated by GTP-bound form of Rac1 GTPase. SCAR/WAVE binds to HSPC300, kette/NAP1 attaches to Sra1/CYFIP1 to form a WAVE complex. C-terminal SH3 domain interacts Abl as well as WASP. Cdc42 in GTP-bound active state directly binds to WASP. WAVE and WASP are regulators of Arp2/3-dependent actin polymerization.

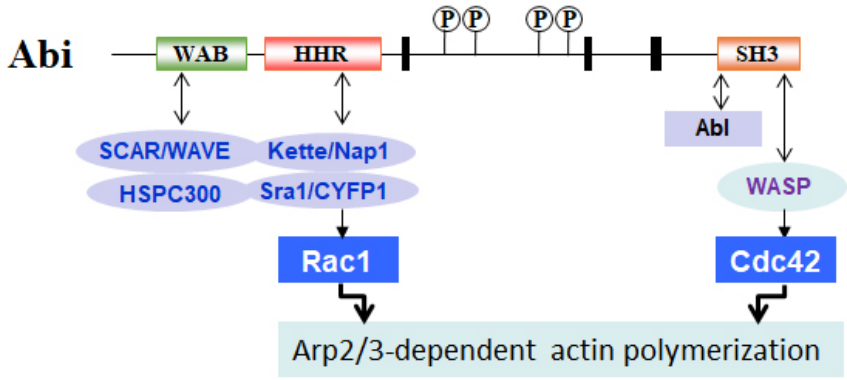
Abi
WAB
HHR
SH3
P
P
P
P
SCAR/WAVE
HSPC300
Kette/Nap1
Sra1/CYFP1
Abl
WASP
Rac1
Cdc42
Arp2/3-dependent actin polymerization

Figure 3. Comparison of Abi proteins between human and fruit fly.

There are three vertebrate Abi family proteins and single homologue in the fly. The mammalian Abi proteins have a similar domain structure to fly Abi with WAB domain, HHR domain, proline-rich regions, and SH3 domain, additional serine/threonine-rich region (SR) and polyproline structure (PP). Amino acid residues are numbered in each protein. (The mammalian Abi domain structures are modified from Sato et al., 2012)

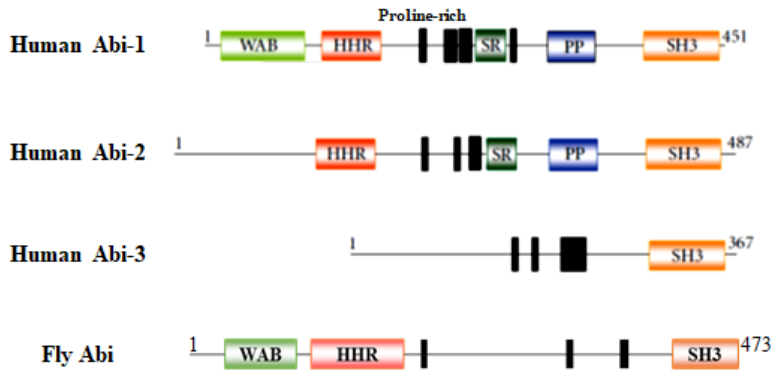
Proline-rich
Human Abi-1
1
WAB
HHR
SR
PP
SH3
451
Human Abi-2
1
HHR
SR
PP
SH3
487
Human Abi-3
1
SH3
367
Fly Abi
1
WAB
HHR
SH3
473

plasma membrane in charge of endocytosis and endosomal sorting (Mooren et al., 2012). Endocytosis is divided into two major pathways, clathrin-dependent endocytosis (CDE) and clathrin-independent endocytosis (CIE). Clathrin-dependent pathway is mediated by the assembly of clathrin to form coated vesicle and by direct binding of adaptor protein-2 (AP-2) complex to clathrin and cargo destined for internalization. Clathrin-independent pathway encompasses the endocytosis that occurs in the absence of clathrin, such as caveolin-dependent endocytosis, GPI-enriched endocytic compartment (GEEC) pathway, phagocytosis, and macropinocytosis. WASP and Arp3 are colocalized with clathrin during initiation of endocytosis in cultured fibroblasts, indicating that WASP and Arp2/3 complex are recruited to sites of clathrin-dependent endocytosis to move a short distance into the cytosol (Merrifield et al., 2004). *Drosophila* Abi regulates bristle formation required with WASP function for F-actin induction (Bogdan et al., 2005). Abi1 is involved in epidermal growth factor receptor (EGFR) endocytosis through WASP and also engaged in ruffle formation and macropinocytosis via WAVE (Innocenti et al., 2005). SCAR/WAVE complex is linked with membrane protrusions such as lamellopodia and filopodia. Moreover, Abi and Rac1-WAVE are critical players in macropinocytosis (Kerr and Teasdale, 2009; Dubielecka et al., 2010; Rottner et al., 2010; Fujii et al., 2013), implicating that Abi is an endocytic molecule. Phosphorylation of Abi by Abl is critical for binding Abi to SCAR complex (Kotula, 2012), suggesting that Abi-Abl-Rac1-WAVE pathway acts in macropinocytosis. Our lab

recently published about Abi-SCAR pathway to regulate synaptic growth (Kim et al., 2019). It demonstrated that Abi, Abl, Rac1 and WAVE are participated in macropinocytic regulation of BMP receptor to attenuate retrograde BMP signaling at the *Drosophila* neuromuscular junction. However, the molecular mechanism of Abi-WASP pathway and their physiological significance remain to be elucidated.

Involvement of chromosomes in reciprocal translocations is the feature of many hematological malignancies. *BCR-ABL1* oncogene, whose role in hematopoiesis has been well defined, is generated by the balanced reciprocal translocation and is associated with CML due to its excessive kinase activity (Quintas-Cardama and Cortes, 2009). Recurrent translocations of human *MLL* (myeloid/lymphoid or mixed-lineage leukemia) gene has been reported to be associated with AML. Abi revealed one of the partner genes of *MLL* in that MLL-ABI chimeric transcripts were detected in bone marrow cells from AML patients (Taki et al., 1998; So et al., 2000; Shibuya et al., 2001). Furthermore, recent studies have discovered that conditional deletion of Abi1 causes MPNs in mouse bone marrow (Chorzalska et al., 2018). Moreover, Abi1 protein and mRNA levels are decreased in hematopoietic progenitors from patients with PMF, but not from those with essential thrombocythemia (ET) or polycythemia vera (PV). These data implicated that Abi has a role in hematopoiesis, yet its function has not been investigated at the organismal level.

3. Purpose of research

As previous reports have suggested that Abi may influence hematopoietic diseases, my research has focused on identifying the role of Abi in hematopoiesis. As a model to this study specifically, the *Drosophila* hematopoietic system has several advantages on the research of blood cells formation, functions, and mechanisms. First of all, compared to other model animals, *Drosophila* is more convenient to analyze in terms of understanding the functions of a specific gene at the individual level and obtaining the mutant or transgenic flies. Additionally, techniques for selectively expressing genes depending on the timing of development or the type of cells are well developed. Thirdly, hemolymph and lymph gland of *Drosophila* consist of myeloid blood cells and are responsible for innate immunity similar to vertebrates. Fourthly, the genes that regulate hematopoiesis and corresponding signal transduction pathway are evolutionarily preserved with vertebrates (Neyen et al., 2014; Zacharioudaki and Bray, 2014; Petraki et al., 2015). With these advantages, the study of genes that regulate hematopoiesis using *Drosophila* provides important clues to understanding the mechanism of human hematopoietic system and associated diseases.

The first specific aim of my research was to discover the direct involvement of Abi in *Drosophila* hematopoiesis. To test this possibility, I examined whether *abi* mutants have defects in hematopoiesis. In addition, I examined the localization of Abi in hemocytes. The second specific aim of my research was to define

the molecular mechanisms that are regulated by Abi. To test this possibility, I examined whether Abi interacts with components of the known signaling during hematopoiesis. Furthermore, I examined whether Abi is required for the regulation of hematopoiesis specific signaling *in vivo* and in cultured cells. Taken together, my research is conducted to clarify the role and to unveil the detailed mechanisms of Abi in hematopoiesis.

Materials and Methods

Fly stocks

Drosophila melanogaster stocks were raised on standard cornmeal-dextrose fly media at 25℃. The wild-type strain using in this study was w^{1118}. The abi^{5}, *UAS-HA-abi*, *UAS-HA-*$abi^{\Delta 30-65}$, *UAS-HA-*$abi^{W452K,}$ and *abi-GAL4* used in the published paper (Kim et al., 2019) were adopted to this study (Figure 4 and Figure 17). Briefly, the *abi* null allele abi^{5} was generated by imprecise excision of G6718 obtained from GenExel (Daejeon, South Korea). Transgenic flies carrying the following constructs were generated in the w^{1118} background using standard procedures: abi^{5}, *UAS-HA-abi*, *UAS-HA-*$abi^{\Delta 30-65}$, *UAS-HA-*$abi^{W452K,}$ and *abi-GAL4.*

Df(3R)su(Hw)7 (a deficiency of the *abi* locus, BDSC 1049), *lz-GAL4*, *UAS-mCD8-GFP* recombinant (BDSC 6314), *eater-GAL4* (BDSC 36322), *NRE-EGFP* (BDSC 30727), *UAS-*$Notch^{RNAi}$*-1* (BDSC 7077), *UAS-*$Notch^{RNAi}$*-2* (BDSC 7078), $Notch^{1}$ (BDSC 6873), *UAS-Nicd* (BDSC 52008), Ser^{1} (BDSC 2537) $WASp^{1}$ (BDSC 51657), $SCAR^{\Delta 37}$ (BDSC 8754), *UAS-*$Cdc42^{T17N}$ (BDSC 6288), $Cdc42^{2}$ (BDSC 9105), *UAS-*$WASp^{RNAi}$ (BDSC 36119), *Df(3R)3450* (a deficiency of the wsp locus, BDSC 7688), *UAS-*$AP\text{-}2\alpha^{RNAi}$ (BDSC 32866), *UAS-*$Rac1^{T17N}$ (BDSC 6292), *UAS-*$SCAR^{RNAi}$ (BDSC 31126), *UAS-*$CtBP^{RNAi}$ (BDSC 31334), *UAS-*$Rabankryin^{RNAi}$ (BDSC 34883), *UAS-*$Graf^{RNAi}$ (BDSC 6426) fly lines were obtained from the Bloomington *Drosophila* Stock Center (BDSC; Bloomington, Indiana, USA). *UAS-*Chc^{RNAi} (VDRC 24789)

fly line was obtained from the Vienna *Drosophila* Resource Center (VDRC; Vienna, Austria). The *srp-GAL4* fly line was kindly provided by Lucas Waltzer (Centre de Biologie du Développement, Toulouse, France). *HmlΔdsRed* fly line was kindly provided by Katja Brückner (University of California San Francisco, San Francisco, California, USA).

Larval staging and analysis

Egg lays took place at 25°C for 6 hours and aged for each developmental time point; AEL 68-74 hours as second instar, AEL 75-81 hours as early third instar, AEL 93-99 hours as mid third instar and AEL 109-115 hours as late third instar larvae at 25°C. Larvae were analyzed in the same number of males and females.

Molecular Biology

For expression in the S2R+ cells, a full-length cDNA (Clone ID: RE42104) for Serrate (CG6127) was from the Drosophila Genomics Resource Center (DGRC; Bloomington, Indiana, USA). The Serrate cDNA was amplified by two-step PCR to generate cDNA with a C-terminal Myc (EQKLISEEDL) tag before the stop codon. The Serrate-Myc cDNA was ligated into the pGEM-T easy vector and then moved into pAc5.1 vector (Invitrogen, Carlsbad, California, USA).

For RNAi experiments in S2-Mt-N cells, *abi*, *Chc*, *Rabankyrin*, *WASp*, and *SCAR* dsRNAs were synthesized by *in vitro* transcription of their cognate DNA templates, as previously

described (Lee et al., 2007). To generate DNA templates, I used primers containing the T7 promoter sequence upstream of the following: *abi*, 5'-GCCTCGCATCGATATTCTA-3' and 5'-ACCATATAGAGCGTATGTG-3'; *Chc*, 5'-GCCTGCTGGAAATGAAT-3' and 5'-CGCTCCACCTCCTTAAT-3'; *Rabankyrin*, 5'-GCCAAATCTAGTTAAGAAG-3' and 5'-GCAGCGGAGATGCCTTATC -3'; *Wasp*, 5'-GATGGTCATGTGGGACTAAA-3' and 5'-GATGGATGAC GGGTTGGCAC-3'; *SCAR*, 5'-GTGTATCAGCAGGATGAGC -3' and 5'-CGCCGTGCACCAGTGCACG-3'.

Hemocyte counting and statistical analysis

For counting total larval hemocytes, circulating hemocytes were first isolated by bleeding and sessile cells were then released by scraping the body wall with a needle under a dissection microscope. The collected hemolymph (~1 μl) was mixed with 9 μl of Schneider's medium containing protease inhibitors (Complete; Roche Life Science, Penzberg, Germany). The hemolymph sample was transferred to a Neubauer improved hemocytometer (Marienfeld, Lauda-Königshofen, Germany) for counting under a light microscope. The collected values were analyzed for normality with the D'Agostino-Pearson omnibus test and used for significance testing. To determine statistical significance, I performed the Student's t-test followed by post hoc pairwise comparisons of means using Tukey-Kramer test.

Live imaging and analysis

For live fluorescent imaging of hemocytes, late third instar larvae were carrying *HmlΔdsRed* were selected under the fluorescence microscope and anesthetized with CO_2. Images were acquired using an Olympus fluorescence microscope.

To acquire the image from live animals, larvae carrying both with *lz-GAL4, UAS-mCD8-GFP* and *HmlΔdsRed* or with *NRE-EGFP* and *HmlΔdsRed* are selected under the fluorescence microscope. Briefly, selected larvae were washed in PBS, dried on filter paper, and placed dorsal side down to confocal dish. Adjusting CO_2 to anesthetize, images were obtained by a Carl Zeiss (Oberkochen, Germany) LSM800 confocal laser scanning microscope using a Plan Apo 20x 0.8 NA objective. For analyze the population of hemocytes undergoing transdifferentiation, Hml and Lz double-positive cells divided Hml-positive cells, both counted within sessile clusters.

Crystal cell visualization and analysis

For visualizing mature crystal cells in the larval stage, late third instar larvae were heated at 70°C for 10 minutes. Crystal cells in the posteriormost abdominal segments A7 and A8 of larvae are counted. Images were obtained with an Olympus BX51 microscope with a DP72 camera (Shinjuku, Tokyo, Japan).

For visualizing embryonic crystal cells, recombinant embryos were generated by carrying *lz-GAL4, UAS-mCD8-GFP* in wild-

type and *abi*^{5}*/Df* background, respectively. Then embryos were fixed and mounted using the SlowFade reagent. Images were obtained by a Carl Zeiss LSM800 confocal laser scanning microscope using a Plan Apo 20x 0.8 NA objective. GFP positive cells located in head mesoderm were counted at stage 17.

Hemocyte immunostaining

For immunofluorescence staining, circulating hemocytes were obtained by bleeding late third instar larvae in a drop of Schneider's medium on a coverslip. After one-hour incubation at room temperature to settle down on a coverslip, the samples were fixed in 4% formaldehyde in PBS for 30 minutes. The hemocytes were washed three times with PBS containing 0.3% Triton X-100 within 10 minutes and blocked with 0.1% BSA in PBS for 10 minutes. The cells were then stained with mouse anti-NimC1 (kindly gifted from Eva Kurucz, Biological Research Center of the Hungarian Academy of Sciences, Szeged, Hungary) at 1:200 or mouse anti-Lz antibody (Developmental Studies Hybridoma Bank, Iowa City, Iowa, USA) at 1:5 overnight at 4°C. The samples were incubated with Cy3-conjugated secondary antibodies (Jackson ImmunoResearch, West Groove, Pennsylvania, USA) at 1:200 for 1 hour at room temperature. A cell nucleus was visualized using DAPI (1:10000, Molecular Probes, Eugene, Oregon, USA).

For determining the Abi expression, larval sessile hemocytes were dissected from mid third instar larvae expressing both *HmlΔdsRed* and *lz-GAL4, UAS-mCD8-GFP* in PBS and fixed in 4%

formaldehyde in PBS for 30 minutes. Fixed samples were washed three times with PBS containing 0.3% Triton X-100 with 10 minutes, blocked with 5% BSA in PBS and incubated with rat anti-Abi antibody at 1:100 (Kim et al., 2019) overnight at 4℃. Samples were incubated with Cy5-conjugated secondary antibodies (Jackson ImmunoResearch) at 1:200 for 1 hour at room temperature.

Stained cells were mounted using the SlowFade reagent (Invitrogen) and imaged with a Carl Zeiss LSM800 confocal laser scanning microscope using a Plan Apo 63x 1.4 NA oil objective.

Cell culture and transient transfections

Drosophila Schneider S2R+ cells were maintained at 25℃ in Schneider's medium (Invitrogen) supplemented with 10% heat-inactivated (30 minutes, 55℃) fetal bovine serum (FBS; Gibco, Gaithersburg, Maryland, USA). S2R+ cells were transfected with C-terminal Myc-tagged Serrate in serum-free medium using Cellfectin according to the manufacturer's instructions.

S2-Mt-N cells were purchased from *Drosophila* Genomics Resource Center (DGRC 154) and were grown in Sang M3 Insect Medium (Sigma, St. Louis, Missouri, USA) supplemented with bacto-peptone, yeast-extract, 10% heat-inactivated FBS, and 2E-7 M methotrexate (Sigma). Expression of Notch under control of metallothionein (MT) promoter in S2-Mt-N cells was induced by the addition of 0.7 mM copper sulfate overnight or 4 mM for 2 hours. Same volume of S2R+ cells and S2-Mt-N cells put together on the

PLL-coated coverslip in cell culture plates and were co-cultured with rotation at 40-50 rpm for 2 hours at room temperature.

Antibody feeding assay

The induced S2-Mt-N cells were incubated with mouse anti- Necd antibody (Developmental Studies Hybridoma Bank) at 1:10 diluted in PBS for 30 minutes on ice for extracellular labeling. Adding the same volume of Serrate-expressing S2R+ cells, the cells were co-cultured at room temperature. After 2 hours, the co-cultured cells were incubated with mouse FITC-conjugated secondary antibodies (Jackson ImmunoResearch) at 1:200 diluted in PBS for 30 minutes. Then samples were fixed in 4% formaldehyde in PBS for 30 minutes, permeablized with PBS containing 0.3% Triton X-100 for 10 minutes and blocked with 0.1% BSA in PBS for 10 minutes. The cells were then immunostained with rabbit anti-Myc antibody (Cell Signaling Technology, Danvers, Massachusetts, USA) at 1:1000 for 1 hour, following stained with both mouse Cy3-conjugated and rabbit Cy5-conjugated secondary antibodies (Jackson ImmunoResearch) at 1:200 for 1 hour at room temperature. Stained cells were mounted using the SlowFade reagent (Invitrogen) and imaged with a Carl Zeiss LSM800 confocal laser scanning microscope using a Plan Apo 63x 1.4 NA oil objective.

Wounding assay

Larvae in late third instar stage were washed in PBS, dried on filter paper and impaled with a 0.1-mm steel needle (Fine Science Tools,

Foster City, California, USA) at the dorsal midline between the hair stripes of abdominal segment A3 or A4 (Galko et al., 2004). After wounding, larvae were returned to fly media and cultured at 25℃ incubator. Melanized larvae were assessed with 10 minutes interval during one hour under a dissection microscope. Images from live wounded animals were obtained with an Olympus BX51 microscope with DP72 camera.

Statistical analysis

All quantitative data are express as the mean values ± s.e.m of at least three experiments. The values were analyzed for normality with the D'Agostino-Pearson omnibus test and used for significance testing. To determine statistical significance, I performed the Student's t-test followed by post hoc pairwise comparisons of means using Tukey-Kramer test.

Figure 4. Molecular characterization of *abi*−null mutant and the region of antigen.

(a) The genomic organization of the *abi* locus at 88A9 on chromosome III and mapping of one *abi*−null mutant. The exon−intron structures of *abi* are shown. White and black boxes represent untranslated and coding regions, respectively. The insertion site of the P−element line G6718 indicated as the inverted triangle in the coding region of *abi*. The extent of the deletion in abi^{5} which was generated by imprecise excision of G6718 are indicated. The abi^{5} allele has a 1075 bp deletion in the second and the third exons of *abi*. The gray bar shows the promoter region used for the generation of the *abi−GAL4* (-2801 ~ -17 bp upstream of the initiator ATG).

(b) RT−PCR analysis of total extracts prepared from the third instar wild−type (WT), abi^{5} (abi^{5}/abi^{5}) and $abi^{5}/Df(3R)su(Hw)7$ (abi^{5}/Df) mutant larvae. mRNA expression of *abi* detects one band at 1422 bp in wild−type animals (WT). This band is not detected in abi^{5} and abi^{5}/Df mutants. The adjacent gene, *twf* (*twinfilin*), is normally expressed in the same samples. *rp49* as a control.

(a) and (b) are modified from Kim et al., 2019.

(c) The gray bar under the schematic domain represents the region against antibody. The C−terminal fragment containing amino acids 253 to 473 was generated for antigen.

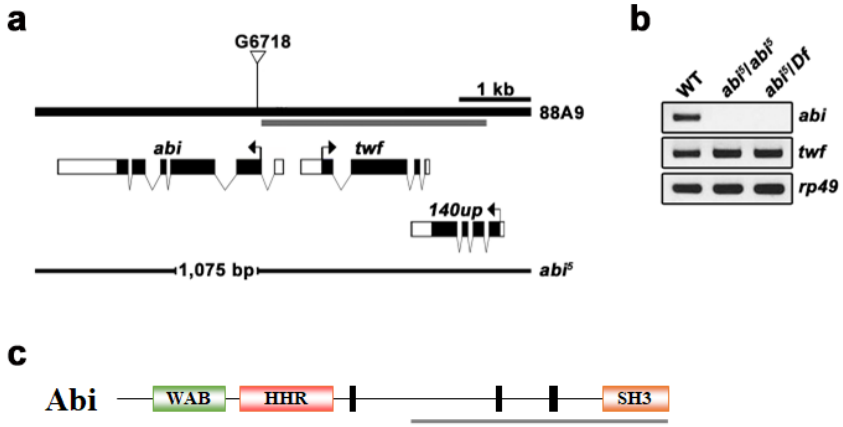
a
G6718
1 kb
88A9
abi
twf
140up
1,075 bp
abi5
b
WT
abi5/abi5
abi5/Df
abi
twf
rp49
c
Abi
WAB
HHR
SH3

Results

1. Loss of Abi leads to hematopoietic defects.

To investigate the role of Abi in hematopoiesis, I analyzed hemocytes population of wild-type and *abi* mutant larvae in late third instar when the last stage of larval hemocyte production at the individual level and as a whole (Lanot et al., 2001). For estimating the total hemocyte population, I quantified the total hemocytes number per larva. The number of total hemocytes per animal was not significantly changed in abi^{5}/Df larvae compared to wild-type (Figure 5a). Observing the total hemocytes with fluorescence visualization using the hemocyte reporter HmlΔ-DsRed (Makhijani et al., 2011), there were no severe alterations of the expression level and distribution of total hemocytes between wild-type and abi^{5}/Df larvae (Figure 5b). Because approximately 95% of the hemocytes are plasmatocytes, these results suggest that Abi does not affect the proliferation of plasmatocytes. To analyze the crystal cell development, I counted the melanized cells in the posterior hematopoietic tissue where the representative region generally examined for the crystal cell population (Kurucz et al., 2007). This region includes the organ referred to as sessile clusters localized between the epidermis and muscle layers. In late third instar stage, abi^{5}/Df larvae demonstrated a reduced number of sessile crystal cells compared to wild-type (Figure 6a and 6b).

Larval sessile hemocytes have dynamics in the terminal cluster attributable to the detachment from the cluster, circulation in

Figure 5. *abi* mutants show a normal range of total hemocyte number and the distribution of plasmatocytes.

(a) The graph represents that number of total hemocytes per larva were not significantly different between wild-type (WT) and *abi* mutant (*abi*^{5}/*Df*) larvae in late third instar stage. 16 larvae were analyzed per each genotype.

(b) Live mount images in late third instar larvae of WT (*HmlΔdsRed*/+, upper) and *abi*^{5}/*Df* (*HmlΔdsRed*/+; *abi*^{5}/*Df*, lower), using the hemocyte reporter HmlΔ-dsRed (HmlΔ>dsRed, red). Note that *abi*^{5}/*Df* larvae did not show severe alterations in expression and distribution of plasmatocytes compared to WT.

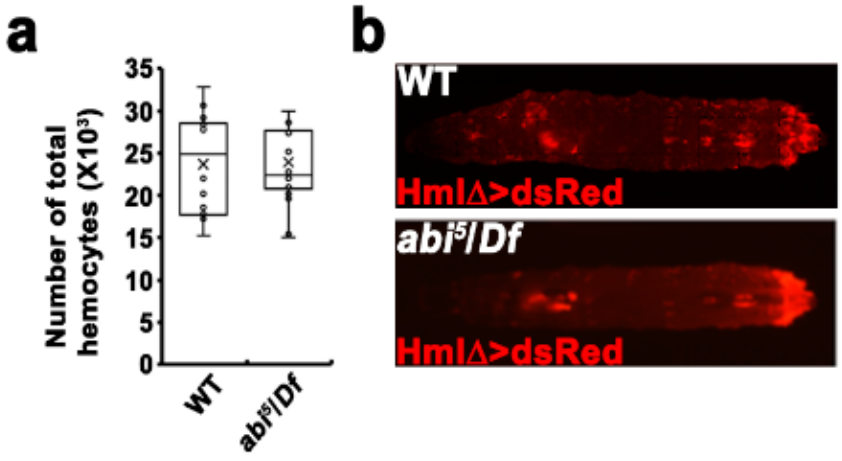
a
Number of total hemocytes (X10³)
35
30
25
20
15
10
5
0
WT
abi⁵/Df
b
WT
HmlΔ>dsRed
abi⁵/Df
HmlΔ>dsRed

Figure 6. *abi* mutants exhibit a reduced number of larval crystal cells.

(a) Images from posterior parts of late third instar larvae of wild-type (WT, left) and *abi* mutant (*abi*^{5}/*Df*) larvae. Scale bar, 100 μm.

(b) The sessile crystal cell numbers of *abi*^{5}/*Df* are decreased compared to WT in late third instar larvae.

(c) Confocal images in circulating hemocytes of WT (left) and *abi*^{5}/*Df* (right) larvae in late third instar stage. The circulating crystal cells are marked by anti-Lz antibody (Lz, red). The nucleus of hemocytes is marked by DAPI (DAPI, blue). Scale bar, 50 μm.

(d) The population of circulating Lz-positive hemocytes of *abi*^{5}/*Df* larvae were decreased compared to WT in late third instar stage.

(b) and (d), 16 larvae were analyzed per each genotype. *P<0.001.

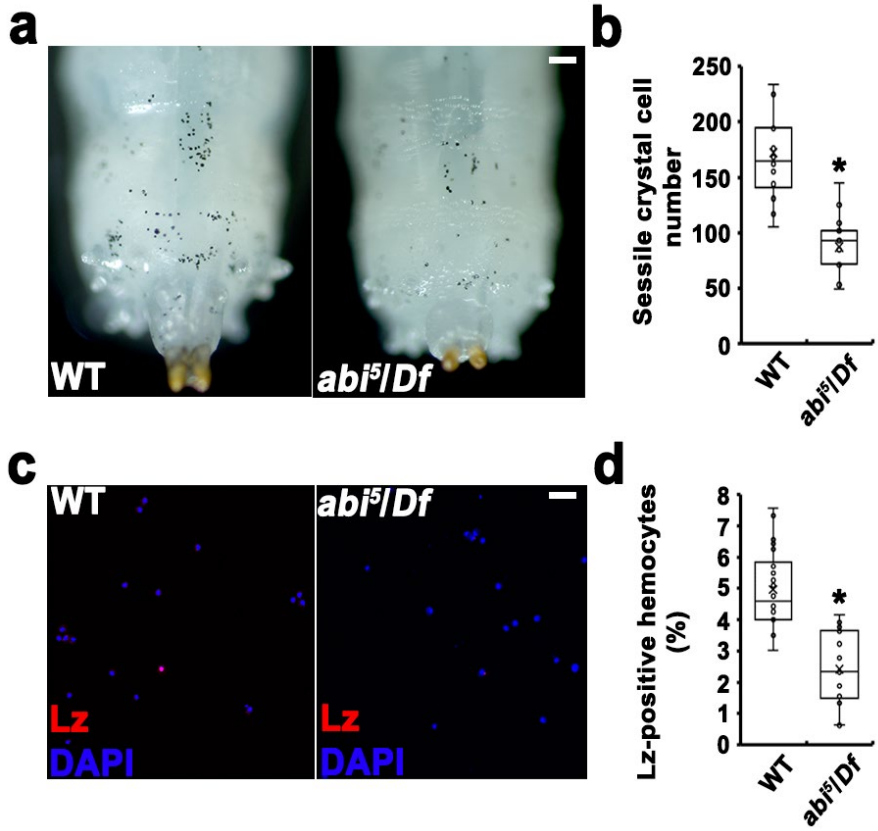
a
WT
abi5/Df
b
Sessile crystal cell number
250
200
150
100
50
0
*
WT
abi5/Df
c
WT
abi5/Df
Lz
DAPI
Lz
DAPI
d
Lz-positive hemocytes (%)
8
7
6
5
4
3
2
1
0
*
WT
abi5/Df

hemolymph, and subsequent re-attachment to sessile sites (Makhijani et al.,2011). To test the possibility that the reduction of crystal cells in the sessile cluster part may induce the elevation of those in the circulating part correspondingly in *abi* mutants, I analyzed the crystal cell population in circulating hemocytes (Bretscher et al., 2015). Antibody staining using the crystal cell marker Lz (Evans et al., 2014) displayed that around 5% Lz-positive hemocytes consist of circulating hemocytes in wild-type larvae as known. However, the population of Lz-positive hemocytes in abi^{5}/Df larvae is also reduced as shown in sessile parts (Figure 6c and 6d). Therefore, *abi* mutants have reduced crystal cell population, both in sessile and circulating hemocytes. Taken together, loss of Abi leads to a reduction of the crystal cell number with no change of total hemocyte population in late third instar larvae.

2. Abi regulates transdifferentiation of plasmatocytes into crystal cells.

2.1. *abi* mutants show normal hemocyte differentiation in embryogenesis.

The crystal cell lineage first originated from Lz-positive hemocytes during embryogenesis. In the embryonic phase of *Drosophila* hematopoiesis, approximately 800 blood cells differentiate from the head mesoderm. Most of these cells become plasmatocytes that migrate throughout the embryo. Hemocytes are first characterized at embryonic stage 5 by the expression of Serpent (Srp) (Lebestky et al., 2000). A complex regulatory circuit involving Srp and Lz functions to both specify crystal cells and also to limit their numbers. Physical interaction between Srp and Lz synergizes to activate and control lz transcription and determines the crystal cell fate. Thus Lz expression can only induce crystal cells in Srp-positive cells and loss of Srp provokes the reduction of Lz expression. Approximately 36 hemocytes are designated as crystal cells and remain in the head mesoderm region of the embryo until larval stages (Milchanowski et al., 2004). At embryonic stage 13, hemocytes undergo a segmented and migrated away from the ventral midline to lateral side (Sánchez-Sánchez et al., 2017). At stage 17, hemocytes are dispersed evenly distributed throughout the embryo (Tepass et al., 1994). To identify the reason of reduced population of larval crystal cells in abi mutants, I analyzed the embryonic crystal cell at stage 17 using larvae carrying Lz-GFP and discovered that abi mutants have the normal population of

embryonic crystal cell number (Figure 7a and 7b). Moreover, I could not observe the defects of hemocyte migration and distribution.

After embryonic development, the hemocyte population expands throughout larval development in both circulation and sessile patches (Leitão and Sucena, 2015). To observe the development of larval crystal cell readily, I analyzed the crystal cell population starting with the second instar stage larvae. The sessile crystal cell numbers between wild-type and abi^{5}/Df were not significantly different in the second instar larvae (Figure 8a). Additionally, the circulating crystal cell population between wild-type and abi^{5}/Df were not significantly altered in the second instar larvae (Figure 8b). However, there were pronounced reductions of crystal cells in the late third instar stage of abi^{5}/Df larvae. Therefore, mutation of *abi* has no problem in Srp-positive hemocyte lineage but, has a problem in next lineage occurred at the larval stages.

2.2. *abi* mutants show a defect in plasmatocyte transdifferentiation.

The second crystal cell lineage occurs in early third instar larval stage (Leitão and Sucena, 2015). Although mature crystal cells do not appear to form new cells by mitosis, certain portions of Hml-positive plasmatocytes within the sessile clusters transformed into Lz-positive crystal cells. This transdifferentiation is validated by the existence of hemocytes having two different cell type

Figure 7. *abi* mutants have the normal crystal cell number in the embryonic stage.

(a) Confocal images in embryonic stage 17 of WT (*lz-GAL4, UAS-mCD8-GFP,* upper panel) and *abi*^{5}/*Df* (*lz-GAL4, UAS-mCD8-GFP/+; abi*^{5}/*Df,* lower panel) embryos. Lz-expressing cells were marked by GFP fluorescence and the cells in white line boxes in the left side were magnified to the right side and counted. Scale bars, 50 μm.

(b) The graph shows Lz-GFP-positive cell number in each genotype embryo at stage 17. There were no differences between WT (*lz-GAL4, UAS-mCD8-GFP*) and *abi*^{5}/*Df* (*lz-GAL4, UAS-mCD8-GFP/+; abi*^{5}/*Df*) embryos. 15 embryos were analyzed per each genotype.

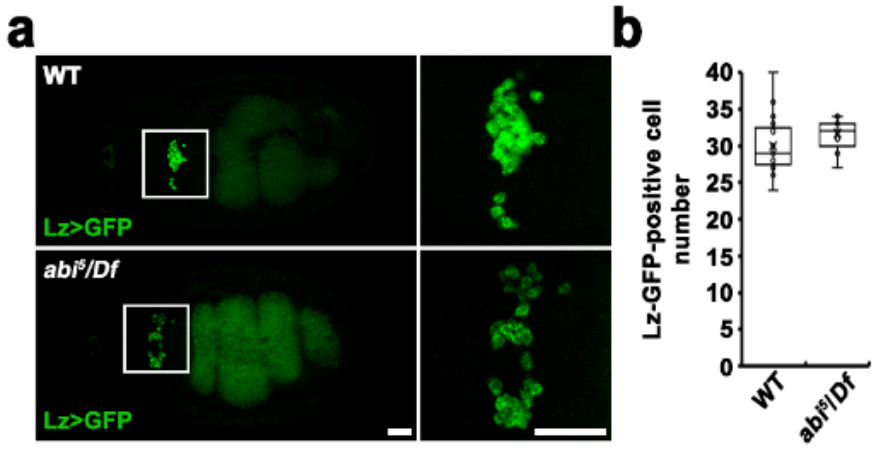
a
WT
Lz>GFP
abi5/Df
Lz>GFP
b
Lz-GFP-positive cell number
40
35
30
25
20
15
10
5
0
WT
abi5/Df

Figure 8. *abi* mutants have the normal crystal cell number in the second instar larval stage.

(a) The graph shows sessile crystal cell number in the second instar larvae of wild-type (WT) and *abi* mutant (*abi*^{5}/*Df*) larvae. The sessile crystal cell numbers between WT and *abi*^{5}/*Df* were not significantly different. 10 larvae were analyzed per each genotype.

(b) The graph shows circulating crystal cell population in the second instar larvae of WT and *abi*^{5}/*Df*. The population of Lz-positive circulating hemocytes in *abi*^{5}/*Df* is not significantly different compared to WT. 16 larvae were analyzed per each genotype.

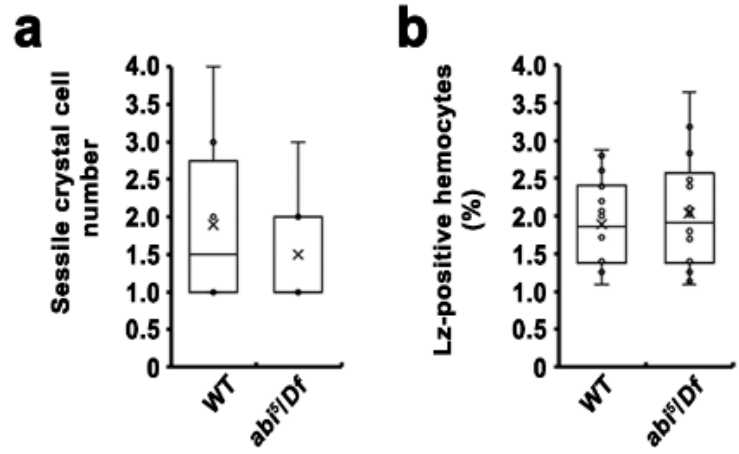
a
Sessile crystal cell number
4.0
3.5
3.0
2.5
2.0
1.5
1.0
0.5
0
WT
abl[5]/Df
b
Lz-positive hemocytes (%)
4.0
3.5
3.0
2.5
2.0
1.5
1.0
0.5
0
WT
abl[5]/Df

markers and contributes to the crystal cell population of the late larval stage. To investigate whether *abi* mutants have problems in this period, I generated the recombinant larvae carrying HmlΔ-dsRed for marking plasmatocytes and Lz-GFP for marking crystal cells in a wild-type and abi^{5}/Df background, respectively. Additionally, I set up confocal microscope specifications to obtain the live image of larvae for this assay. In early third instar stage, small portions of Lz-positive crystal cells show up in the cluster of Hml-positive plasmatocytes. At this stage, plasmatocyte cluster and Lz-positive crystal cell population of abi^{5}/Df larvae seem to be the same with those of wild-type larvae (Figure 9a). In the process of development, Hml-positive plasmatocytes are expanded by their self-mitotic activity. Both wild-type and abi^{5}/Df larvae have normal plasmatocytes clusters (Figure 9d). In late third instar stage, Lz-positive crystal cells are also increased in their number accompanied by an increase of hemocytes containing both Hml-positive and Lz-positive markers in wild-type larvae. However, Lz-positive crystal cells are relatively decreased in their number in abi^{5}/Df larvae (Figure 9b and 9c late L3). Moreover, the quantification of the Hml- and Lz-positive hemocytes (Hml+Lz+) displayed that the population of double positive hemocytes is remarkably reduced in abi^{5}/Df larvae compared to control. As a result, Abi regulates the process of plasmatocytes transdifferentiation into crystal cells.

Figure 9. Loss of Abi impairs transdifferentiation of plasmatocytes to crystal cells.

(a) Live mount confocal images of the sessile cluster hemocytes in early third instar larvae (early L3). Left column represents of WT larva (*lz-GAL4, UAS-mCD8-GFP/+; +/HmlΔdsRed*) and right column shows abi^{5}/Df larva (*lz-GAL4, UAS-mCD8-GFP/+; +/HmlΔdsRed;* abi^{5}/Df). Hml-positive cells (HmlΔ>dsRed, upper, red) are plasmatocytes and Lz-positive cells (Lz>GFP, middle, green) are crystal cells. The lower row for merged channels.

(b) Live mount confocal images of the sessile cluster hemocytes in late third instar larvae (late L3). Left column shows of WT larva (*lz-GAL4, UAS-mCD8-GFP/+; +/HmlΔdsRed*) and right column represents abi^{5}/Df larva (*lz-GAL4, UAS-mCD8-GFP/+; +/HmlΔdsRed;* abi^{5}/Df). The upper row exhibits Hml-positive plasmatocytes (HmlΔ>dsRed, red), the middle row shows Lz-positive crystal cells (Lz>GFP, green), and the lower row for merged channels. Note that less of Lz-positive cells in abi^{5}/Df compared to WT.

(a) and (b), Scale bars, 50 μm.

(c) The graph shows that quantified absolute number of hemocytes undergoing transdifferentiation. Hml and Lz double-positive cells are counted within sessile clusters. Note that Hml and Lz double-positive cells were reduced in late third instar (late L3), not in early third instar (early L3) of abi^{5}/Df larva.

(d) The graph exhibits that analyzed absolute number of Hml-positive hemocytes counted within sessile clusters. Note that there

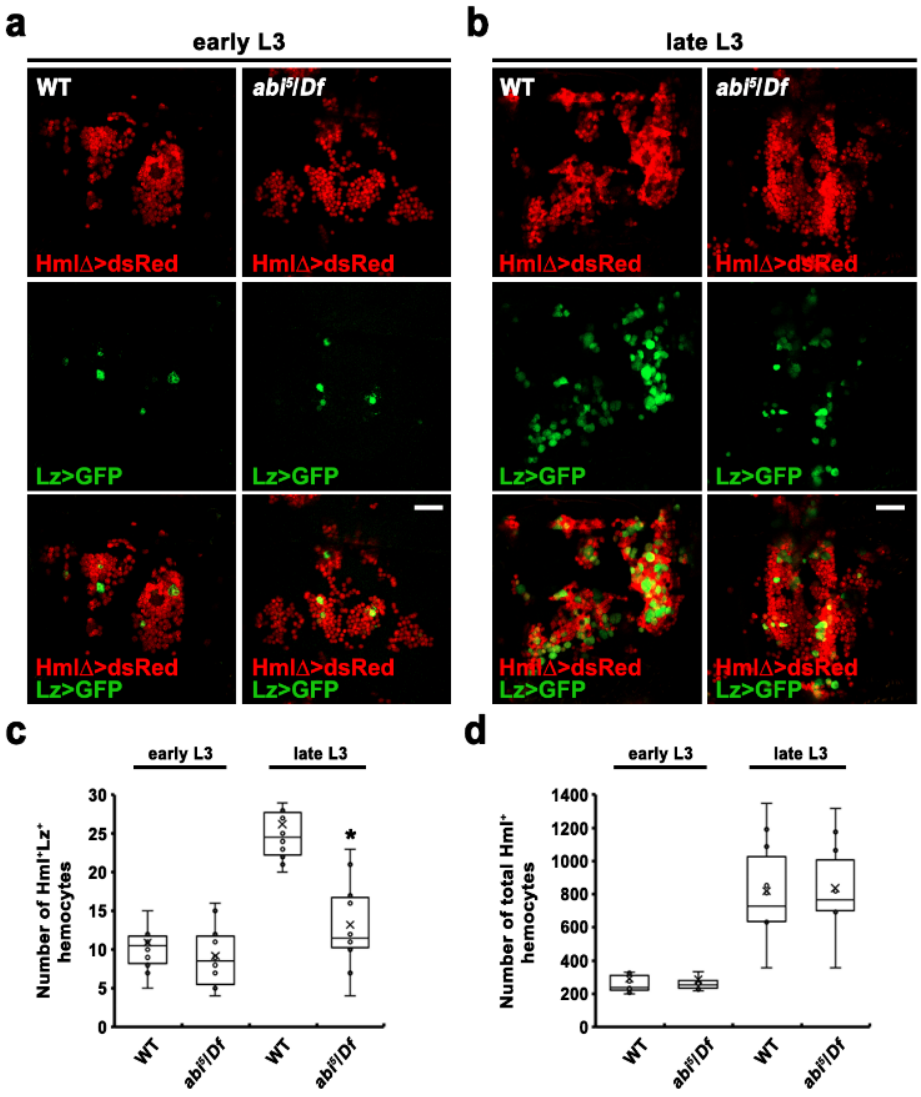
a
early L3
WT
abl5/Df
HmlΔ>dsRed
Lz>GFP
b
late L3
c
Number of Hml+Lz+ hemocytes
d
Number of total Hml+ hemocytes
WT
abl5/Df

was no significant difference of Hml−positive plasmatocytes between WT and *abi*^{5}/*Df* larva, both in early third instar (early L3) and late third instar (late L3) stage.

(c) and (d), 10 larvae were analyzed per each genotype. *P<0.001.

3. Abi is required for the crystal cell differentiation in larval stages.

To determine Abi function in regulating crystal cells, I attempted to rescue the phenotypes observed in *abi*^{5}/*Df* larvae by expressing Abi protein through the GAL4-upstream activating sequence (UAS) system in the *abi* mutant background (Brand and Perrimon, 1993). There are three different kinds of GAL4 drivers that I used for rescue experiments. All hemocytes express the GATA factor Serpent (Srp) (Rehorn et al. 1996), making *srp-GAL4* a universal hemocyte-specific driver (Brückner et al., 2004). Since *srp-GAL4* drives from embryonic circulating cells, stage and cell type specific GAL4 were necessary to determine the roles of Abi in plasmatocyte transdifferentiation. Therefore, I selected the *eater-GAL4* (Tokusumi et al., 2009) given it is expressed by plasmatocytes and activated during the second instar stage (Kroeger et al., 2013). The last one is *abi-GAL4* made up with *abi* promoter to determine whether Abi functions on hemocytes.

When Abi was expressed with a hemocyte driver *srp-GAL4* in *abi*^{5}/*Df* background, I observed full rescue activity for the sessile crystal cell number and the circulating crystal cell population (Figure 10). This result signifies that prohemocyte-specific expression of Abi influences the crystal cell differentiation. In addition, when Abi was expressed with a plasmatocyte driver *eater-GAL4* in *abi*^{5}/*Df* background, I found the sessile crystal cell number and circulating crystal cell population were restored to wild-type levels. This result exhibits that plasmatocyte-specific

Figure 10. Abi is required for positive regulation of the crystal cell differentiation.

(a) Images from posterior parts of late third instar larva of wild-type (WT, left), *abi*^{5}/*Df* (middle) and *srp-GAL4/+; abi*^{5}/*UAS-HA-Abi,Df* (srp>Abi rescue, right). Scale bar, 100 μm.

(b) The graph shows sessile crystal cell number in late third instar larvae of indicated genotypes. Expression of Abi in all hemocytes by using *srp-GAL4* (srp>Abi rescue) was rescued *abi*^{5}/*Df* larva phenotype compared to control (srp>control, *srp-GAL4/+*). When Abi was expressed with *eater-GAL4* in *abi*^{5}/*Df* background (eater>Abi rescue, *eater-GAL4,abi*^{5}/*UAS-HA-Abi,Df*), the sessile crystal cell number were restored to control levels (eater>control, *eater-GAL4/+*). Abi was expressed with an *abi-GAL4* in *abi*^{5}/*Df* background (abi>Abi rescue, *abi-GAL4/+; abi*^{5}/*UAS-HA-Abi,Df*), sessile crystal cells were increased very close to GAL4 control value (abi>control, *abi-GAL4/+*).

(c) The graph shows circulating crystal cell population in late third instar larvae of indicated genotypes. Expression of Abi in all hemocytes (srp>Abi rescue) was rescued *abi*^{5}/*Df* larva phenotype compared to control (srp>control). Abi was expressed with *eater-GAL4* in *abi*^{5}/*Df* background (eater>Abi rescue), restoring the crystal cell population to control levels (eater>control). Abi was expressed with an *abi-GAL4* in *abi*^{5}/*Df* background (abi>Abi rescue), increasing the crystal cell population very close to GAL4 control value (abi>control).

(b) and (c), 16 larvae were analyzed per each genotype. *P<0.001.

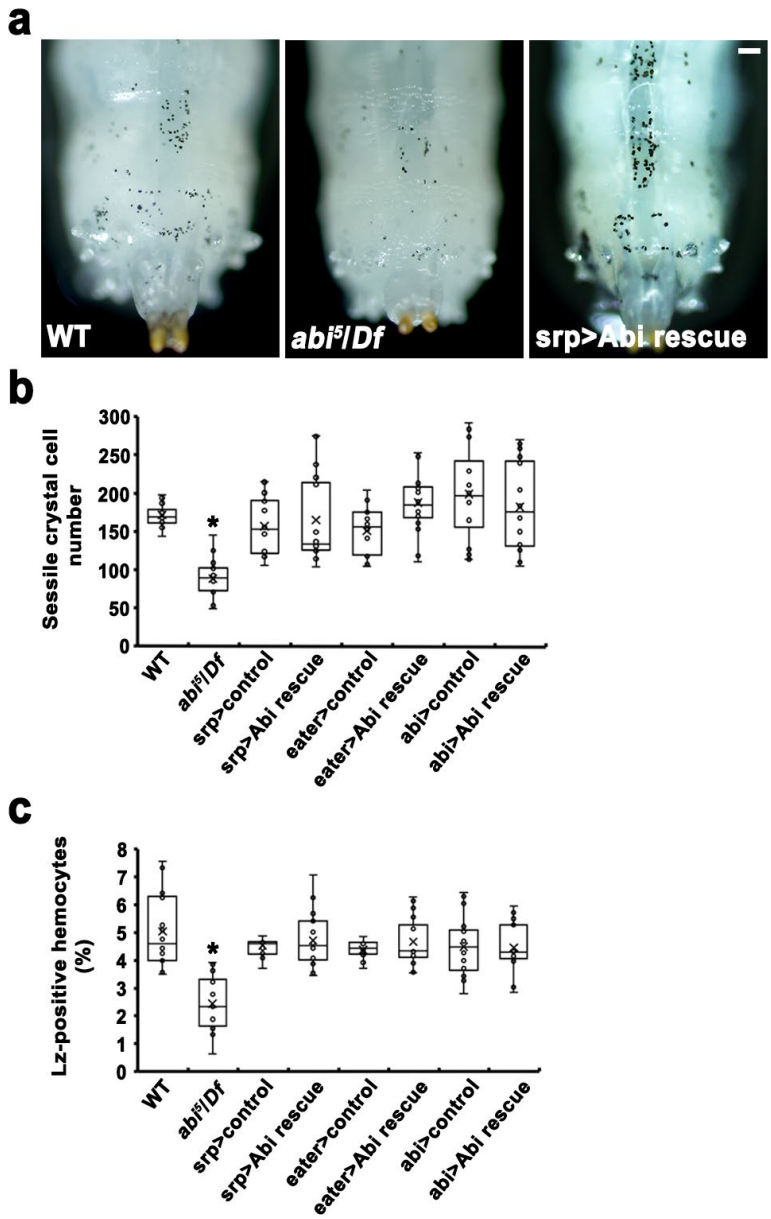
a
WT
abi5/Df
srp>Abi rescue
b
Sessile crystal cell number
300
250
200
150
100
50
0
WT
abi5/Df
srp>control
srp>Abi rescue
eater>control
eater>Abi rescue
abi>control
abi>Abi rescue
c
Lz-positive hemocytes (%)
8
7
6
5
4
3
2
1
0
WT
abi5/Df
srp>control
srp>Abi rescue
eater>control
eater>Abi rescue
abi>control
abi>Abi rescue

expression of Abi in the second instar stage has an effect on the regulation of the crystal cell population in the third instar stage. Furthermore, when Abi was expressed with an *abi-GAL4* in abi^{5}/*Df* background, I discovered that crystal cells were increased very close to wild-type value in rescued larvae, meaning that Abi acts in hemocyte to regulate the crystal cell population. Collectively, Abi is required for the crystal cell differentiation in larval stages.

4. Determination of the Abi expression in hemocytes.

Loss-of-function mutation in *abi* induced the defects in the crystal cell development, and the phenotypes were rescued by expressing Abi under the control of *abi-GAL4* driver. These results required additional studies to confidently note hematopoietic defects are a cell-autonomous function of Abi. These experiments were performed by determining Abi expression on hemocytes. To detect the expression patterns of Abi, I performed immunostaining with anti-Abi antibody using the larvae carrying both HmlΔ-dsRed and Lz-GFP. As a result, Abi is expressed in Hml-positive plasmatocytes and also expressed in Lz-positive crystal cells in circulating hemocytes (Figure 11a). In the abi^{5}/Df background, Abi signal could not be detected on both cell types. Next, UAS-GFP reporter line was driven by *abi-GAL4* to evaluate the *abi*-GAL4 expression. Plasmatocytes are marked by anti-Nimrod C1 (NimC1), and antibody against Lz is used for marking crystal cells. GFP expression was observed in NimC1-positive plasmatocyte and Lz-positive crystal cells in circulating hemocytes. These expression data demonstrate that the Abi acts cell-autonomously to regulate the differentiation of hemocytes.

Figure 11. Abi is expressed in both plasmatocytes and crystal cells.

(a) Confocal images of circulating hemocytes in late third instar larval stage of wild-type carrying *lz-GAL4, UAS-mCD8-GFP/+; +/HmlΔdsRed* (WT, upper) and abi^{5}/Df carrying *lz-GAL4, UAS-mCD8-GFP/+; +/HmlΔdsRed;* abi^{5}/Df (abi^{5}/Df, lower). The first column displays Abi-expressing cells with anti-Abi antibody (Abi, blue), the second column for Hml-positive plasmatocytes (HmlΔ>dsRed, red), the third column represents Lz-positive crystal cells (Lz>GFP, green) and the fourth column for merged channels. White dashed lines indicate cell boundary. Note that Abi was expressed in both types of hemocytes. The immunoreactivity of Abi antibody was not detected in abi^{5}/Df larvae.

(b) Confocal images of circulating hemocytes in late third instar larva carrying *abi-GAL4/+; +/UAS-mCD8-GFP*. The first column shows NimC1 (upper, red) or Lz (lower, red), the second column exhibits GFP expression driven by *abi-GAL4* (abi>GFP, green), the third column for merged channels. Note that *abi-GAL4* was expressed in NimC1-positive plasmatocyte (upper) and Lz-positive crystal cells (lower).

(a) and (b), Scale bars, 5 μm.

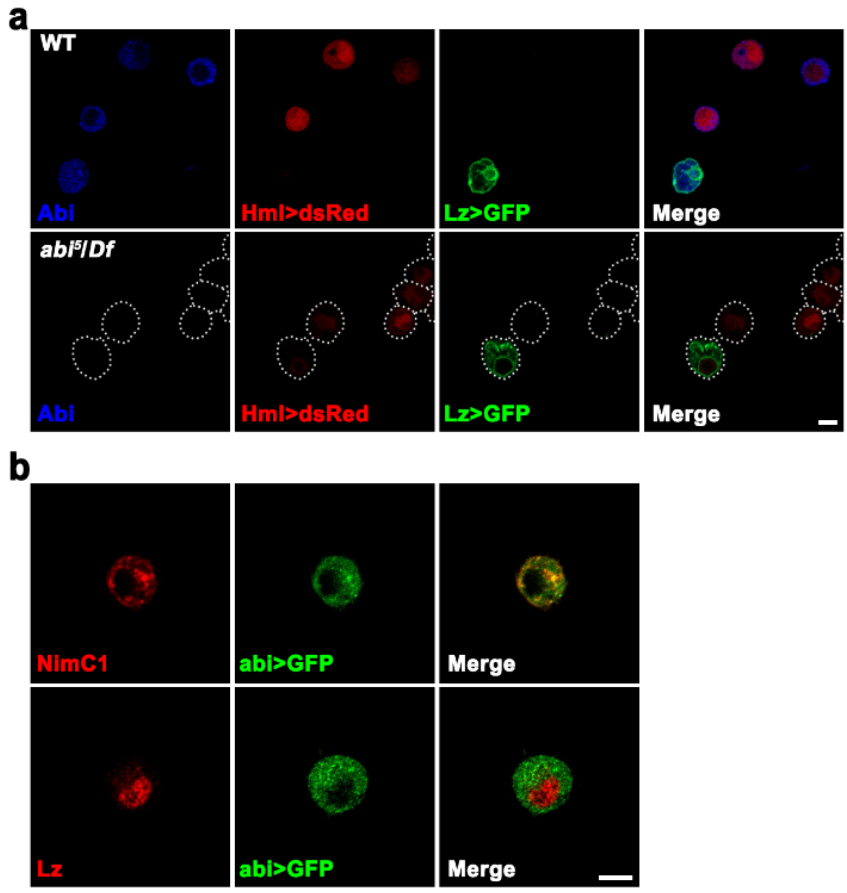
a
WT
Abi
Hml>dsRed
Lz>GFP
Merge
abi5/Df
Abi
Hml>dsRed
Lz>GFP
Merge
b
NimC1
abi>GFP
Merge
Lz
abi>GFP
Merge

5. Abi positively regulates Notch signaling.

The hematopoietic phenotypes shown in *abi* mutants resulted from the impairment of plasmatocyte transdifferentiation, which occurs in larval hematopoietic pockets. Notch signaling has been well studied in the crystal cell development and recently identified as a key signaling in plasmatocyte transdifferentiation. Notch has two ligands, Serrate and Delta, but only the Serrate is working in the crystal cell development (Leitão and Sucena, 2015). Notch signaling in this process started in early third instar stage and consequentially affects the crystal cell population of late third instar stage. To figure out whether the transdifferentiation defect shown in *abi* mutants was due to alteration of Notch signaling, I used the Notch enhancer GFP reporter fly line which enables the detection of active Notch signaling *in vivo* (Furriols and Bray, 2001).

To investigate whether *abi* mutants have an issue in Notch signaling, I generated the recombinant larvae carrying both HmlΔ-dsRed for marking plasmatocytes and Notch responsible element (NRE)-EGFP for marking Notch activated cells in a wild-type and abi^{5}/Df background, respectively. Live confocal images of the mid third instar larvae carrying HmlΔ-dsRed and NRE-EGFP showed that most of the NRE-positive hemocytes are Hml-positive plasmatocytes (Figure 12a). In *abi* mutants, however, there were a very few NRE-positive hemocytes, resulting in the decrement of double positive (Hml-positive and NRE-positive) hemocytes in hematopoietic pockets (Figure 12b). In addition, the intensity of

Figure 12. Loss of Abi leads to the reduction of Notch signaling in sessile hemocytes.

(a) Live mount confocal images of the sessile cluster hemocytes in WT larva carrying genes with *HmlΔdsRed/NRE-EGFP* (WT, upper) and abi^{5}/Df larva carrying genes with *HmlΔdsRed/NRE-EGFP;* abi^{5}/Df (abi^{5}/Df, lower). Note that a very few hemocytes of NRE-positive and weak intensity of their fluorescence in abi^{5}/Df larva, resulting in the decrement of double positive (Hml-positive and NRE-positive) hemocytes in hematopoietic pockets of abi^{5}/Df larva. Scale bar, 10 μm.

(b) The graph shows the quantified number of NRE-positive hemocytes counted within sessile clusters. Note that NRE-positive cells were reduced in abi^{5}/Df larva compared to WT. 16 larvae were analyzed per each genotype. *P<0.001.

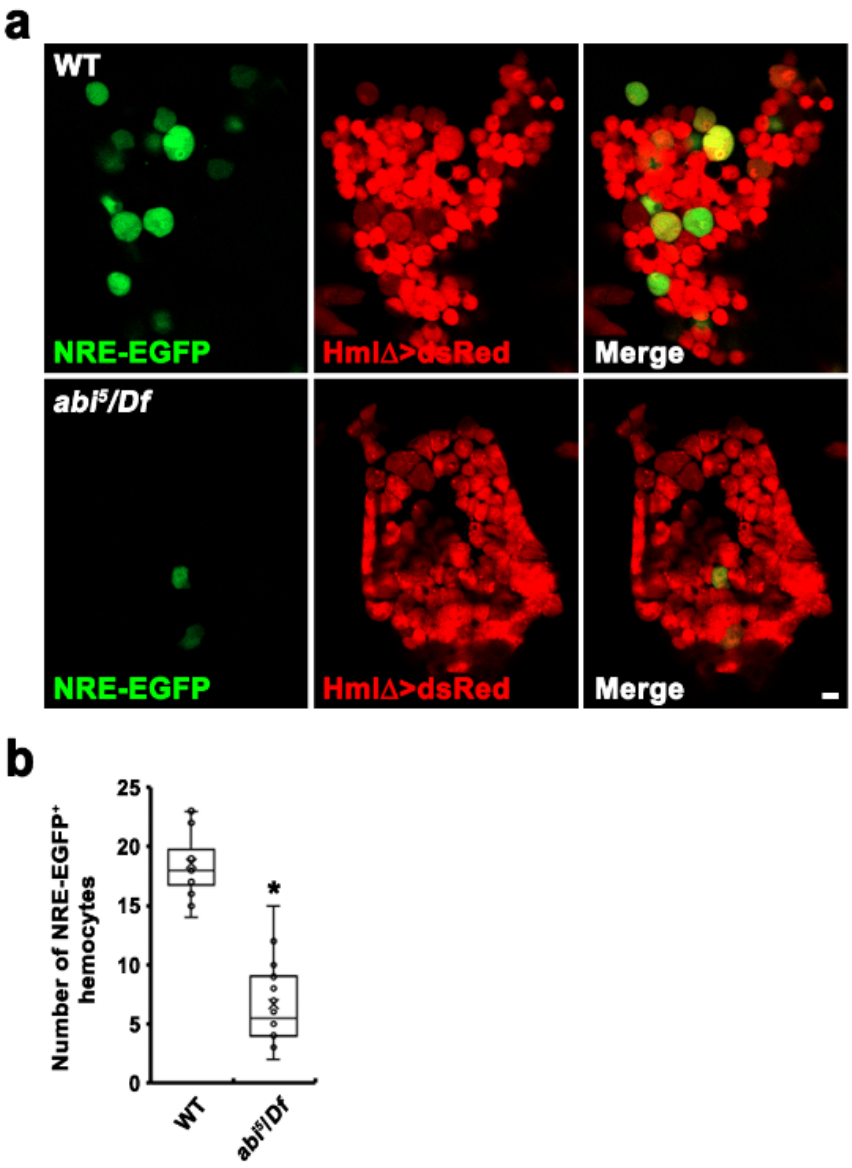
a
WT
NRE-EGFP
HmlΔ>dsRed
Merge
abi5/Df
NRE-EGFP
HmlΔ>dsRed
Merge
b
Number of NRE-EGFP+ hemocytes
25
20
15
10
5
0
*
WT
abi5/Df

NRE-EGFP fluorescence was weak in *abi* mutants. In conclusion, loss of Abi leads to downregulation of Notch signaling. These data suggest that Abi regulates larval plasmatocyte transdifferentiation via positive modulation of Notch signaling.

6. Genetic interaction between *abi* and *notch* for regulating crystal cell population.

6.1. *notch* loss-of-function mutations show hematopoietic defects.

There is evidence that sessile crystal cells are reduced in *notch* temperature-sensitive mutant larva (Duvic et al., 2002). This phenotype was the same as that of *abi* mutants. To mimic the mutant situation, I used two lines of Notch RNAi for knockdown of Notch expression. To analyze the stage-specific phenotype of *notch* knockdown, *srp-GAL4* and *eater-GAL4* were used for these experiments.

Hemocyte-specific knockdown of Notch with *srp-GAL4* induced the decrement of sessile crystal cells as previously reported and the population of Lz-positive circulating hemocytes are also reduced during knockdown of Notch (Figure 13). Moreover, plasmatocyte-specific knockdown of Notch with *eater-Gal4* also showed a severe decrease of sessile crystal cells (Figure 14a and 14b) and Lz-positive circulating hemocytes (Figure 14c), accompanied with no change of total hemocytes number (Figure 14d) alike when knockdown of Notch with *srp-GAL4*. Thus, I confirmed that *notch* loss-of-function mutations show similar phenotypes of *abi* mutants. These results suggested that Abi and Notch contribute to larval crystal cell development during the larval stages.

Figure 13. Depletion of Notch in embryonic stage exhibits a reduction of crystal cells.

(a) Images from posterior parts of late third instar larvae of *srp-GAL4/+* (Control, left), *srp-GAL4/+; +/UAS-Notch^{RNAi}-1* (srp>N^{RNAi}-1, middle) and *srp-GAL4/UAS-Notch^{RNAi}-2* (srp>N^{RNAi}-2, right). Scale bar, 100 μm.

(b) The graph represents sessile crystal cell number in late third instar larvae of indicated genotypes. Note that prohemocyte-specific knockdown of Notch (srp>N^{RNAi}-1, srp>N^{RNAi}-2) showed a reduction of sessile crystal cells compared to *srp-GAL4* control (srp>control).

(c) The graph represents circulating crystal cell population in late third instar larvae of indicated genotypes. Note that prohemocyte-specific knockdown of Notch (srp>N^{RNAi}-1, srp>N^{RNAi}-2) exhibited a reduction of Lz-positive cells compared to *srp-GAL4* control (srp>control).

(d) Number of total hemocytes per larva was not significantly different between srp>control, srp>N^{RNAi}-1 and srp>N^{RNAi}-2.

(b-d),16 larvae were analyzed per each genotype. *P<0.001.

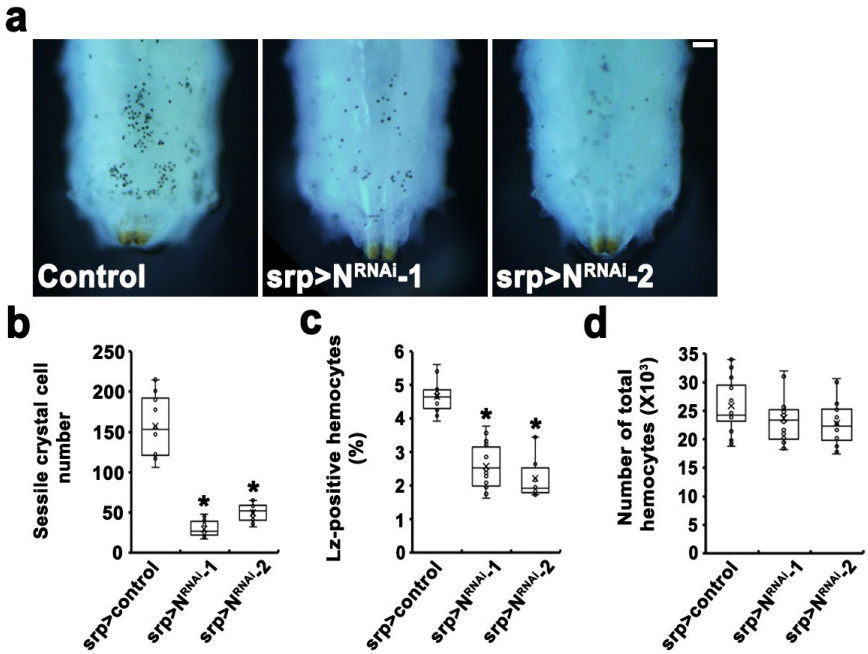
a
Control
srp>N^RNAi-1
srp>N^RNAi-2
b
Sessile crystal cell number
250
200
150
100
50
0
srp>control
srp>N^RNAi-1
srp>N^RNAi-2
c
Lz-positive hemocytes (%)
6
5
4
3
2
1
0
srp>control
srp>N^RNAi-1
srp>N^RNAi-2
d
Number of total hemocytes (X10³)
35
30
25
20
15
10
5
0
srp>control
srp>N^RNAi-1
srp>N^RNAi-2

Figure 14. Plasmatocyte-specific depletion of Notch exhibits a reduction of crystal cells.

(a) Images from posterior parts of late third instar larvae of *eater-GAL4/+* (Control, left), *eater-GAL4/UAS-Notch^{RNAi}-1* (eater>N^{RNAi}-1, middle) and *UAS-Notch^{RNAi}-2/+; +/eater-GAL4* (eater>N^{RNAi}-2, right). Scale bar, 100 μm.

(b) The graph represents sessile crystal cell number in late third instar larvae of indicated genotypes. Note that plasmatocyte-specific knockdown of Notch (eater>N^{RNAi}-1, eater>N^{RNAi}-2) showed a reduction of sessile crystal cells compared to *eater-GAL4* control (eater>control).

(c) The graph displays circulating crystal cell population in late third instar larvae of indicated genotypes. Note that plasmatocyte-specific knockdown of Notch (eater>N^{RNAi}-1, eater>N^{RNAi}-2) exhibited a reduction of Lz-positive cells compared to *eater-GAL4* control (eater>control).

(d) Number of total hemocytes per larva was not significantly different between eater>control, eater>N^{RNAi}-1 and eater>N^{RNAi}-2.

(b-d) 16 larvae were analyzed per each genotype. *P<0.001; **P<0.01.

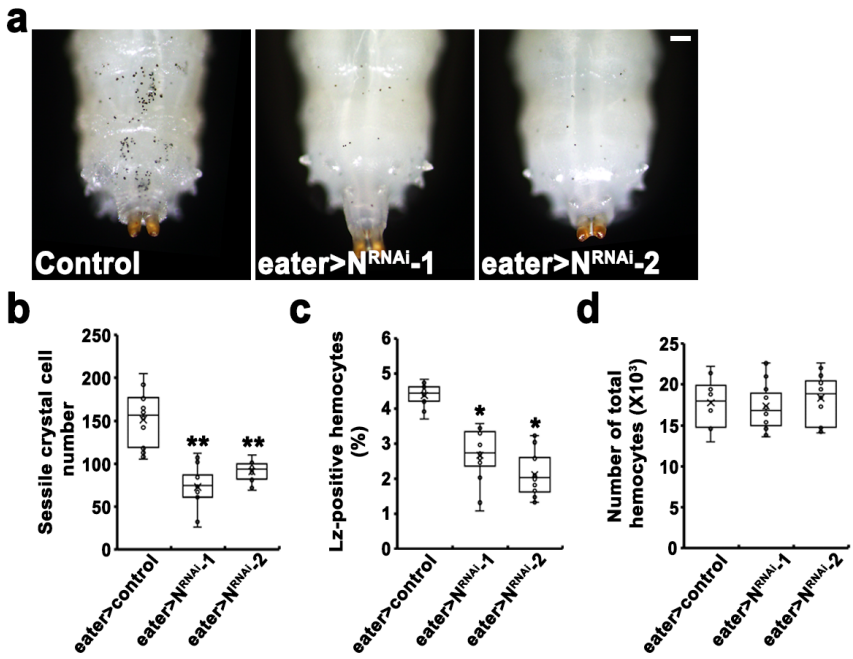
a
Control
eater>N^RNAi-1
eater>N^RNAi-2
b
Sessile crystal cell number
250
200
150
100
50
0
**
**
eater>control
eater>N^RNAi-1
eater>N^RNAi-2
c
Lz-positive hemocytes (%)
6
5
4
3
2
1
0
*
*
eater>control
eater>N^RNAi-1
eater>N^RNAi-2
d
Number of total hemocytes (X10^3)
25
20
15
10
5
0
eater>control
eater>N^RNAi-1
eater>N^RNAi-2

6.2. abi genetically interacts with notch to regulate crystal cell population.

To discover the correlation between Notch and Abi, I investigated the genetic interaction between two genes. Studies on genetic interaction in *Drosophila* have traditionally been known for generating transheterozygous mutants (Price et al., 1997). The one copy deletion of *abi* mutant ($abi^{5}/+$) and one copy deletion of notch mutant ($notch^{1}/+$) caused no change in sessile crystal cell number. However, the double mutant having one *abi* mutant and one *notch* mutant led to reduction of sessile crystal cell number same as *abi* or *notch* mutants (Figure 15a and 15b). This means that *abi* and *notch* work together in the same pathway.

It has been known that the high level expression of Notch by hemocyte-specific GAL4 induces the overgrowth of the crystal cell (Leitão and Sucena, 2015). In my experiments, overexpression of Notch with *srp-GAL4* enhanced the increment of crystal cells in direct opposition to knockdown expression of Notch. However, deleting *abi* gene dose completely suppressed the Notch-driven overproduction of crystal cells (Figure 15c and 15d). I also performed the experiment with *eater-GAL4* to selectively express genes depending on the timing of development and the type of cells. Overexpression of Notch with *eater-GAL4* promoted the increase of crystal cell production as well. Importantly, the overpopulation of crystal cells in Notch gain-of-function mutation was suppressed by deleting the *abi* gene (Figure 15e and 15f).

Notch receptor on the plasma membrane undergoes endocytic

Figure 15. *abi* genetically interacts with *notch* to regulate crystal cell population.

(a) The graph represents sessile crystal cell number in late third instar larvae of indicated genotypes. The $abi^{5}/+$ and $Notch^{1}/+$ larvae showed a normal range of sessile crystal cell number. Note that $Notch^{1}/+; abi^{5}/+$ exhibited the reduced sessile crystal cells.

(b) The graph shows circulating crystal cell population in late third instar larvae of indicated genotypes. The $abi^{5}/+$ and $Notch^{1}/+$ did not significantly change in the crystal cell population. Note that $Notch^{1}/+; abi^{5}/+$ rarely exhibited Lz-positive cells.

(c) The graph represents sessile crystal cell number in late third instar larvae of indicated genotypes. Prohemocyte-driven Notch overexpression (*srp-GAL4/+;+/UAS-N*) exhibited an increase in sessile crystal cell number compared to control (*srp-GAL4/+*). Note that Notch induced crystal cell overproduction was suppressed by decreasing *abi* gene dose ($srp\text{-}GAL4/+; abi^{5}/UAS\text{-}N,Df$).

(d) The graph displays that prohemocyte-driven Notch overexpression (*srp-GAL4/+;+/UAS-N*) exhibited an increase in circulating crystal cell compared to control (*srp-GAL4/+*). However, this phenotype was suppressed by removing of *abi* gene ($srp\text{-}GAL4/+; abi^{5}/UAS\text{-}N,Df$).

(e) The graph shows sessile crystal cell number in late third instar larvae of indicated genotypes. Plasmatocyte-driven Notch overexpression (*eater-GAL4/UAS-N*) exhibited an increase in sessile crystal cell number compared to control (*eater-GAL4/+*). Note that overproduction of crystal cells induced by Notch

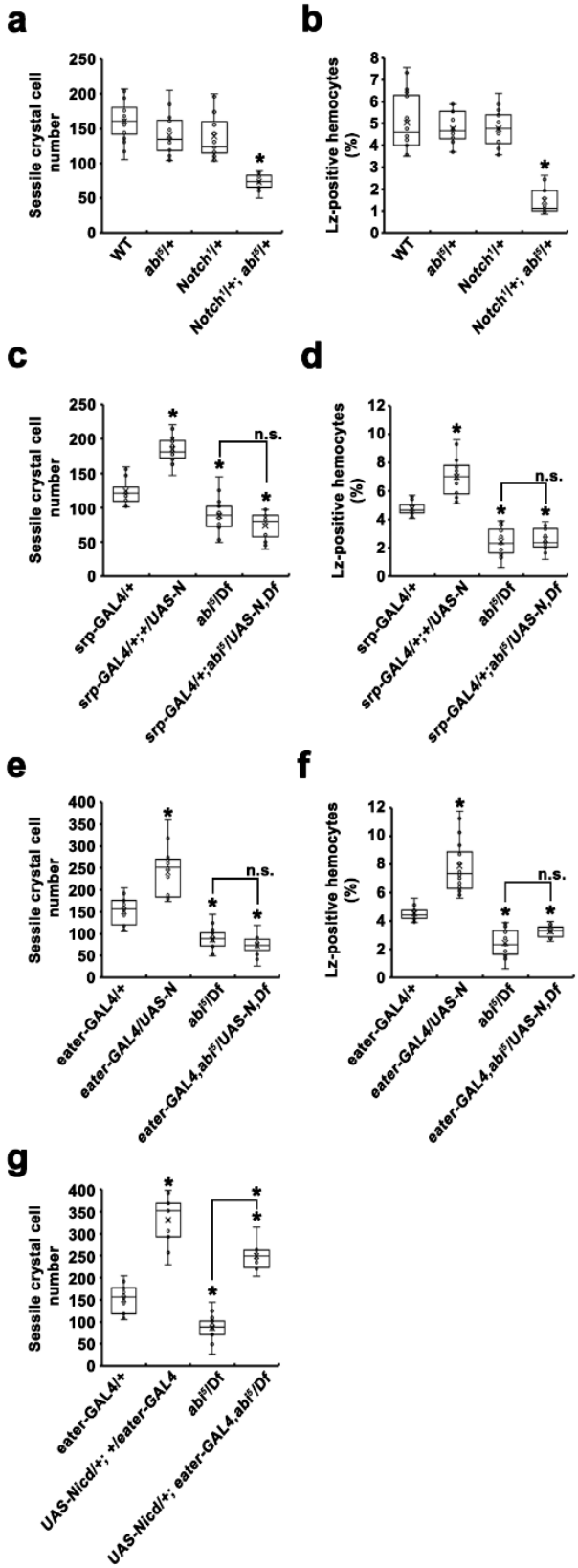
a
Sessile crystal cell number
250
200
150
100
50
0
*
WT
abF/+
Notch1/+
Notch1/+; abF/+
b
Lz-positive hemocytes (%)
8
7
6
5
4
3
2
1
0
*
WT
abF/+
Notch1/+
Notch1/+; abF/+
c
Sessile crystal cell number
250
200
150
100
50
0
*
*
*
*
n.s.
srp-GAL4/+
srp-GAL4/+;+/UAS-N
abF/Df
srp-GAL4/+;abF/UAS-N,Df
d
Lz-positive hemocytes (%)
12
10
8
6
4
2
0
*
*
*
*
n.s.
srp-GAL4/+
srp-GAL4/+;+/UAS-N
abF/Df
srp-GAL4/+;abF/UAS-N,Df
e
Sessile crystal cell number
400
350
300
250
200
150
100
50
0
*
*
*
*
n.s.
eater-GAL4/+
eater-GAL4/UAS-N
abF/Df
eater-GAL4,abF/UAS-N,Df
f
Lz-positive hemocytes (%)
12
10
8
6
4
2
0
*
*
*
*
n.s.
eater-GAL4/+
eater-GAL4/UAS-N
abF/Df
eater-GAL4,abF/UAS-N,Df
g
Sessile crystal cell number
400
350
300
250
200
150
100
50
0
*
*
*
*
*
eater-GAL4/+
UAS-Nicd/+; +/eater-GAL4
abF/Df
UAS-Nicd/+; eater-GAL4,abF/Df

overexpression was suppressed by reduction of *abi* gene (*eater-GAL4,abi*^{5}/*UAS-N,Df*).

(f) The graph represents that plasmatocyte expression of Notch resulted in overproduction of crystal cells (*eater-GAL4/UAS-N*) compared to control (*eater-GAL4/+*). However, knockout of *abi* gene suppressed the overpopulation of crystal cells driven by Notch overexpression (*eater-GAL4,abi*^{5}/*UAS-N,Df*).

(g) The graph shows sessile crystal cell number in late third instar larvae of indicated genotypes. Expression of Notch intracellular domain (Nicd) in plasmatocytes increased crystal cell number both wild-type (*UAS-Nicd/+*; *+/eater-GAL4*) and *abi*^{5}/*Df* genetic background (*UAS-Nicd/+*; *eater-GAL4,abi*^{5}/*Df*).

(a-g) 16 larvae were analyzed per each genotype. *P<0.001; n.s., not significant.

pathway for translocation of its intracellular domain (Nicd) to the nucleus, the final process of the signaling. This feature of Notch signaling enables that expression of the fragment Nicd makes Notch gain-of-function without endocytic regulation. Specific expression of Nicd in plasmatocytes induce the dramatic increase of sessile crystal cell number (Figure 15g). Surprisingly, plasmatocyte expression of Nicd rescued the decrement of crystal cells in *abi* mutants (Figure 15g). These data indicate that Abi interacts with Notch by endocytosis to regulate crystal cell differentiation.

6.3. Abi functions in Serrate-dependent Notch signaling to differentiate crystal cells.

Serrate is known to be the only ligand for Notch in plasmatocyte transdifferentiation because mutants of Serrate, not Delta and Deltex, reduced numbers of crystal cells (Duvic et al., 2002). Moreover, plasmatocyte specific expression of Serrate RNAi reduced the crystal cell number similar to knockdown of Notch (Leitão and Sucena, 2015). To confirm the ligand specificity, I further investigated the genetic interaction between *abi* and *serrate*. One copy deletion of *serrate* mutant ($Ser^{1}/+$) caused no change in sessile crystal cell number, but double mutant having one *abi* mutant and one *serrate* mutant ($abi^{5}, +/+, Ser^{1}$) led to reduction of sessile crystal cell number (Figure 16). This suggests the relationship between Abi and Serrate during crystal cell development.

Figure 16. *abi* and *serrate* work together in crystal cell differentiation.

The graph displays sessile crystal cell number in late third instar larvae of indicated genotypes. Note that double mutant having one *abi* mutant and one *serrate* mutant (abi^{5},+/+,Ser^{1}) led to a reduction of sessile crystal cell number. 16 larvae were analyzed per each genotype. ***P<0.05.

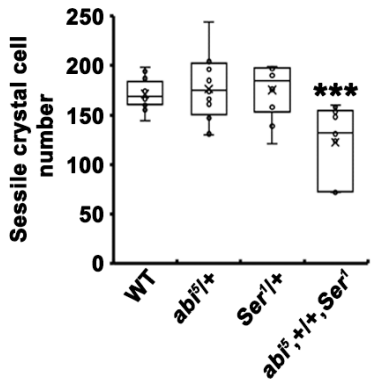
Sessile crystal cell number
250
200
150
100
50
0
***
WT
abl^5/+
Ser^1/+
abl^5,+/+,Ser^1

7. Abi and WASp interaction for maintaining sessile crystal cell population.

7.1. Interaction with WASp via SH3 domain is required for Abi function.

Abi has several domains that can be possible to interact with other proteins (Figure 2). It directly binds to SCAR via its N-terminal WAB domain (Kunda et al., 2003; Echarri et al., 2004), also interacts with WASp through its C-terminal SH3 domain (Bogdan et al., 2005; Innocenti et al., 2005). Partnering with SCAR or WASp, Abi is known to play a role in actin regulation (Stradal et al., 2001).

To reveal which actin regulator is required for the Abi function in the regulation of crystal cell population, I performed rescue experiments with the mutant form of each domain. Deletion of 30 to 65 amino acid residues in the WAB domain ($Abi^{\Delta 30-65}$) is a mutant form of Abi that has impaired binding with SCAR/WAVE complex (Figure 17). Substitution of a single residue of tryptophan 452 to lysine in the SH3 domain (Abi^{W452K}) cannot bind to the WASp protein. The expression of domain mutants of Abi was controlled by *eater-GAL4* for their stage- and cell type-specific expression. There was a correlation between the populations of sessile crystal cells and circulating crystal cells, I analyzed sessile crystal cell and found the phenotypic similarity to *abi* mutants. Expressing Abi with the deletion of 30-65 amino acid under the control of *eater-GAL4* driver ($Abi^{\Delta 30-65}$ rescue) fully rescued the defect in sessile crystal cell population (Figure 18a and 18b). Thus, WAB domain is not involved in the crystal cell development. Expressing Abi with the

tryptophan substitution under the control of *eater-GAL4* driver (Abi^{W452K} rescue) partially rescued the defect in the crystal cell population (Figure 18a and 18b). This means that Abi needs its SH3 domain to participate in crystal cell development. Therefore, Abi and WASP interaction is required for the regulation of sessile crystal cells.

7.2. Abi and WASp are genetically interacted for sustaining sessile crystal cell population.

To discover whether Abi and WASp interactions affected the crystal cell development, I investigated the genetic interaction between the *abi* and *WASp* genes. In addition, it was confirmed that the Abi-SCAR interaction has effects on the crystal cell phenotype. Loss of one copy of *abi*^{5}, *WASp*^{1} and *scar*$^{\Delta 37}$ has a normal range of sessile crystal cell number (Figure 19a and 19b). However, transheterozygous larvae carrying one *abi* mutant and one *WASp* mutant exhibited the reduced sessile crystal cell (Figure 14a and 14b). Additionally, transheterozygous combinations of one *abi* mutant and one *scar* mutant showed the increase of sessile crystal cell (Figure 19a and 19b). In conclusion, Abi interacts with WASp to maintain sessile crystal cell number.

Figure 17. Schematic representation of domain mutations in Abi.

The diagrammatic structures of the deletion and point-mutation form of Abi protein used in this study. Deletion of 30-65 amino acid in WAB domain has a binding defect to SCAR protein ($Abi^{\Delta 30-65}$). Substitution of a single residue of tryptophan 452 to lysine in the SH3 domain cannot interact with the WASp protein (Abi^{W452K}). The single asterisks denote substitution mutations. Amino acid residues are numbered in each form of protein.

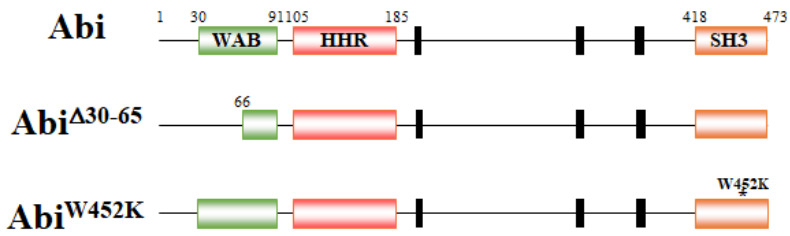
Abi
1
30
91
105
185
418
473
WAB
HHR
SH3
Abi^Δ30-65
66
Abi^W452K
W452K

Figure 18. C-terminal SH3 domain of Abi contributes to the crystal cell differentiation.

(a) Images from posterior parts of late third instar larvae of indicated genotypes. Scale bar, 100 μm.

(b) The graph represents sessile crystal cell number in late third instar larvae of indicated genotypes. Note that expressing Abi with the mutation in SH3 domain under the control of *eater-GAL4* driver (eater>Abi^{W452K} rescue) partially rescued the defect in the crystal cell population. 16 larvae were analyzed per each genotype. *P<0.001; ***P<0.05.

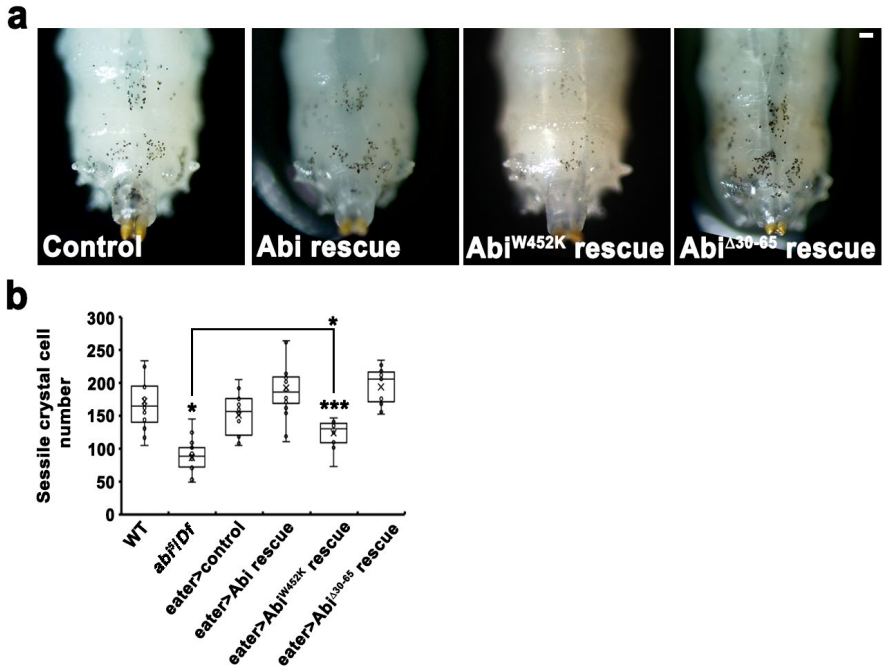
a
Control
Abi rescue
Abi^W452K rescue
Abi^Δ30-65 rescue
b
Sessile crystal cell number
300
250
200
150
100
50
0
*
*
***
WT
abi^5/Df
eater>control
eater>Abi rescue
eater>Abi^W452K rescue
eater>Abi^Δ30-65 rescue

Figure 19. Abi and WASp are genetically interacted for sustaining sessile crystal cell population.

(a) Images from posterior parts of late third instar larvae of indicated genotypes. Scale bar, 100 μm.

(b) The graph represents sessile crystal cell number in late third instar larvae of indicated genotypes. Note that $abi^{5}/+$, $WASp^{1}/+$ and $SCAR^{\Delta 37}/+$ has a normal range of sessile crystal cell number. However, $abi^{5}, +/+, WASp^{1}$ exhibited a reduced sessile crystal cell. $SCAR^{\Delta 37}/+$; $abi^{5}/+$ showed the increase of sessile crystal cell. 16 larvae were analyzed per each genotype. *P<0.001; **P<0.01.

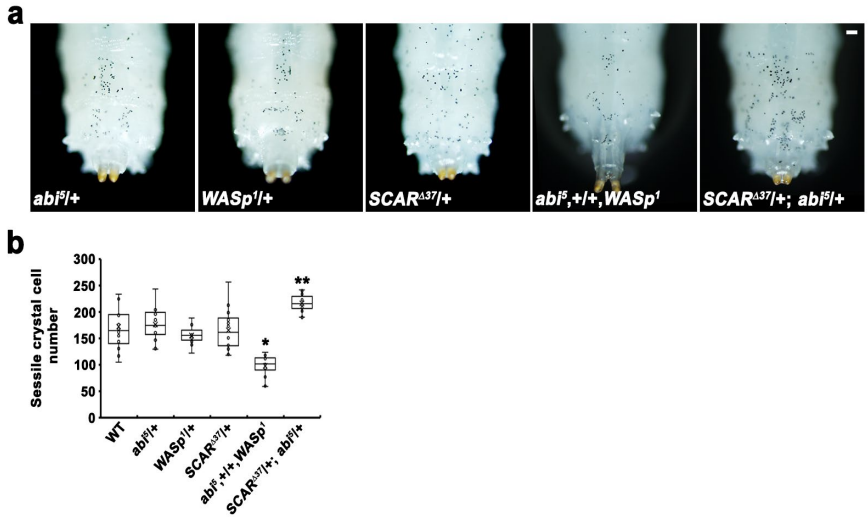
a
abi5/+
WASp1/+
SCARΔ37/+
abi5,+/+,WASp1
SCARΔ37/+; abi5/+
b
Sessile crystal cell number
300
250
200
150
100
50
0
**
*
WT
abi5/+
WASp1/+
SCARΔ37/+
abi5 +/+,WASp1
SCARΔ37/+; abi5/+

8. Clathrin-dependent endocytosis is required for Abi-mediated Notch signaling.

Endocytosis is primarily divided into clathrin-dependent endocytosis and clathrin-independent endocytosis that require the dynamics of filamentous actin structures at the plasma membrane. Abi has been well studied in the field of actin regulation but rarely studied for their roles in endocytosis. Recently, studies discovered that Abi plays a role in micropinocytosis through SCAR complex to regulate synaptic growth. Depending on my data, however, Abi is engaged in hematopoiesis through WASp, not SCAR. Mammalian N-WASP acts as an Arp2/3 activator and triggers actin polymerization during clathrin-dependent endocytosis (Merrifield et al., 2004). It is not yet investigated whether Abi and WASp are directly involved in clathrin-dependent endocytosis. To investigate which endocytic pathway is regulated by Abi in hematopoiesis, I examined the effects on sessile crystal cell differentiation with systematically knockdown of known genes that components of different endocytosis in plasmatocytes. I obtained the mutant or RNAi lines of the components of each pathway and assayed the phenotypic similarity.

8.1. Depletion of WASp-mediated CDE leads to a reduction of crystal cell population.

The WASp protein is an effector of Cdc42 GTPase, which is critical for active assembly in constitutively active state. In my studies, I performed experiments to evaluate whether Cdc42 plays a role in

hematopoiesis. Compared with *eater-GAL4* control, plasmatocyte-specific overexpression of Cdc42 dominant negative form (Cdc42-T17N) decreases sessile crystal cell number (Figure 20a and 20b). Compared with wild-type, $Cdc42^{2}$ mutant displayed reduced sessile crystal cell number (Figure 20c and 20d). These results supported the idea that Cdc42 is involved in crystal cell differentiation. To evaluate the role of the *WASp* gene in hematopoiesis, *WASp* mutants were also analyzed to the crystal cell population. Compared to wild-type, reduced sessile crystal cell number showed in $WASp^{1}/Df$ larvae (Figure 21a and 21b). To confirm this phenotype, I tested the WASp RNAi line to analyze crystal cell population during transdifferentiation. Expression of *UAS-WASp-RNAi* under the control of *eater-GAL4* induced the reduction of both sessile crystal cells (Figure 21c and 21d) and circulating Lz-positive cells (Figure 21e) with no change of total hemocyte population (Figure 21f). Thus, WASp has a function in hematopoiesis to regulate crystal cell population.

To verify the hypothesis that Abi-WASp interaction stimulating actin assembly finally regulates clathrin-dependent endocytosis, the RNAi line of clathrin heavy chain (Chc) is analyzed in hemocytes, since *Chc* mutant homozygote has lethality during the embryonic stage. Plasmatocyte-specific knockdown of Chc caused a dramatic reduction of sessile crystal cells (Figure 22a and 22b). The AP-2 complex plays a major role in clathrin-coated vesicle formation and consists of AP-2α, AP-1-2β, AP-2μ and AP-2σ subunits in fruit fly (Choudhury et al., 2016). Plasmatocyte-

Figure 20. Alteration of Cdc42 expression leads to crystal cell differentiation defect.

(a) Images from posterior parts of late third instar larvae of *eater-GAL4/+* (Control, left) and *eater-GAL4/UAS-Cdc42-T17N* ($Cdc42^{T17N}$, right).

(b) The graph represents that plasmatocyte-specific overexpression of Cdc42 dominant negative form (eater>$Cdc42^{T17N}$) decreased sessile crystal cell number, compared to control (eater>control).

(c) Images from posterior parts of late third instar larva of wild-type (WT, left) and $Cdc42^{2}$ (right).

(d) The graph represents that mutation of Cdc42 led to a reduction in the number of crystal cells.

(a) and (c), Scale bars, 100 μm.

(b) and (d), 16 larvae were analyzed per each genotype. *P<0.001.

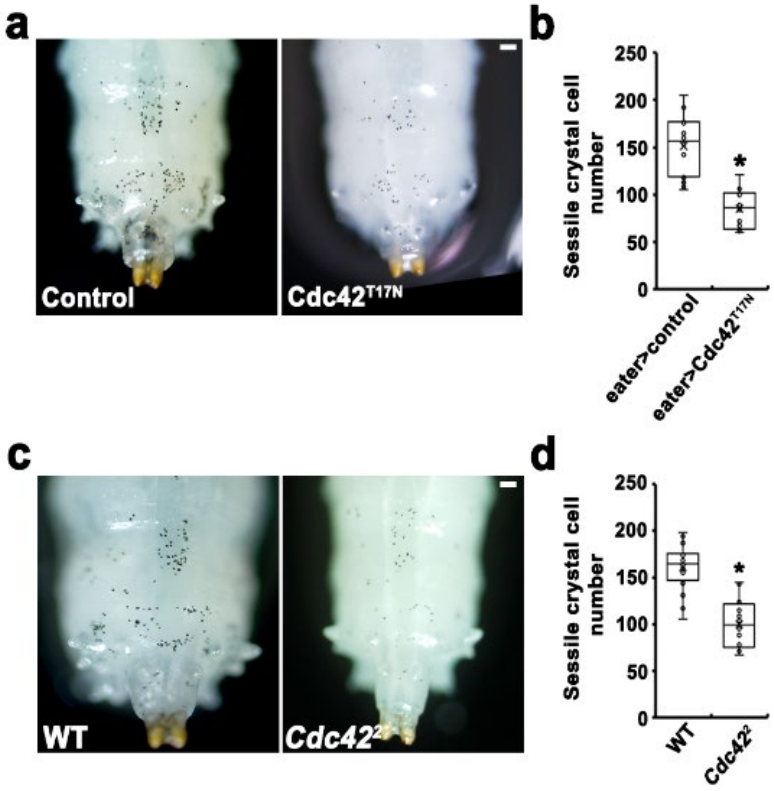
a
Control
Cdc42T17N
b
Sessile crystal cell number
250
200
150
100
50
0
*
eater>control
eater>Cdc42T17N
c
WT
Cdc42
d
Sessile crystal cell number
250
200
150
100
50
0
*
WT
Cdc42

Figure 21. Depletion of WASp leads to a reduction in the number of crystal cells.

(a) Images from posterior parts of late third instar larva of wild-type (WT, left) and *WASp*^{1}/*Df* (right).

(b) The graph represents that depletion of WASp led to a reduction in the number of crystal cells.

(c) Images from posterior parts of late third instar larvae of *eater-GAL4/+* (Control, left) and *eater-GAL4/UAS-WASp-RNAi* (WASp^{RNAi}, right).

(d) The graph shows that expression of *UAS-WASp*-RNAi under control of *eater-GAL4* induced the reduction of sessile crystal cells.

(e) The graph exhibits that Lz-positive hemocyte population decreased in knockdown of WASp compared to control.

(f) The graph displays that the number of total hemocytes per larva between control and knockdown of WASp was not significantly different.

(a) and (c), Scale bars, 100 μm.

(b), (d), (e), and (f), 16 larvae were analyzed per each genotype.

*P<0.001; **P<0.01.

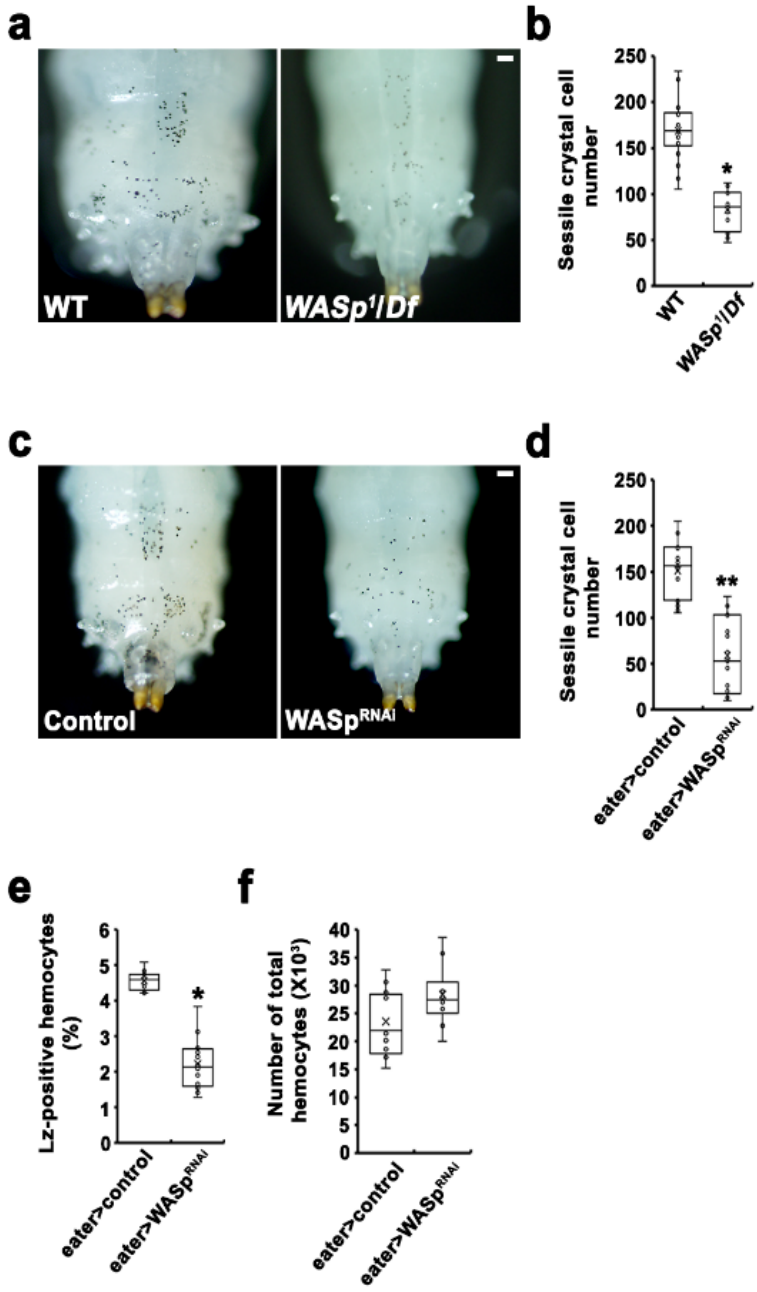
a
WT
WASp1/Df
b
Sessile crystal cell number
250
200
150
100
50
0
*
WT
WASp1/Df
c
Control
WASpRNAi
d
Sessile crystal cell number
250
200
150
100
50
0
**
eater>control
eater>WASpRNAi
e
Lz-positive hemocytes (%)
6
5
4
3
2
1
0
*
eater>control
eater>WASpRNAi
f
Number of total hemocytes (X10³)
40
35
30
25
20
15
10
5
0
eater>control
eater>WASpRNAi

Figure 22. Impairment of Chc and AP-2α expression reduces sessile crystal cell differentiation.

(a) Images from posterior parts of late third instar larvae of *eater-GAL4/+* (Control, left), *eater-GAL4/UAS-Chc-RNAi* (Chc^{RNAi}, middle), and *eater-GAL4/UAS-AP-2α-RNAi* ($AP-2\alpha^{RNAi}$, right). Scale bar, 100 μm.

(b) The graph represents that plasmatocyte-specific knockdown of *Chc* and *AP-2α* induced the defect in the differentiation of sessile crystal cells.

(c) The graph displays that the population of Lz-positive cells decreased in knockdown of *Chc* and *AP-2α* compared to control.

(d) The graph exhibits that total hemocytes number per larva was not significantly different between control and knockdown of *Chc* and *AP-2α*.

(b-d) 16 larvae were analyzed per each genotype. *P<0.001.

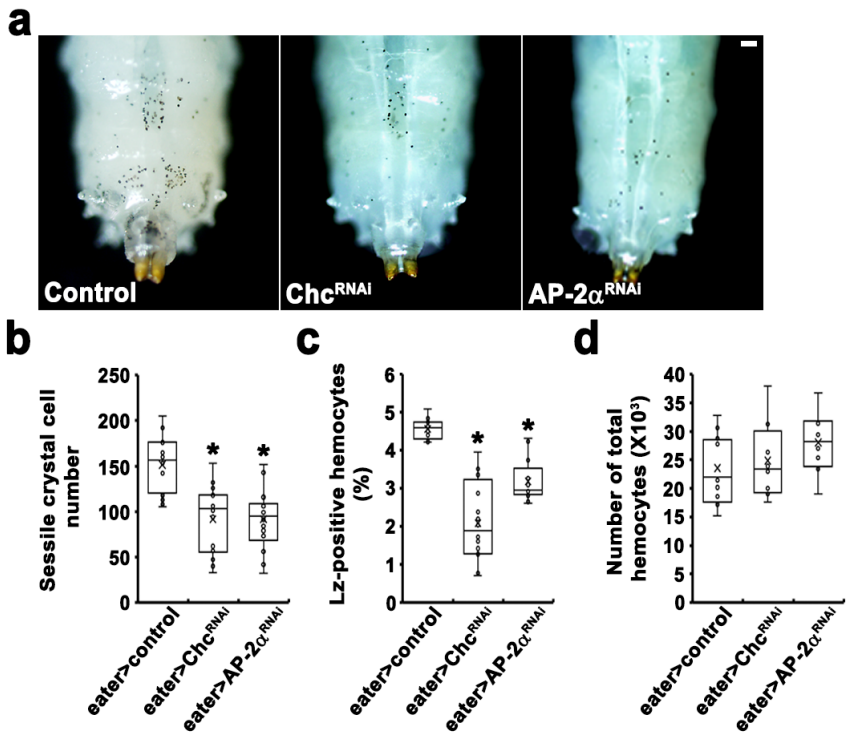
a
Control
Chc^RNAi
AP-2α^RNAi
b
Sessile crystal cell number
250
200
150
100
50
0
*
*
eater>control
eater>Chc^RNAi
eater>AP-2α^RNAi
c
Lz-positive hemocytes (%)
6
5
4
3
2
1
0
*
*
eater>control
eater>Chc^RNAi
eater>AP-2α^RNAi
d
Number of total hemocytes (X10³)
40
35
30
25
20
15
10
5
0
eater>control
eater>Chc^RNAi
eater>AP-2α^RNAi

specific knockdown of each subunit, especially *AP-2α* gene showed a reduction of sessile crystal cells, compared with the control (Figure 22a and 22b). Knockdown of AP-1-2β, AP-2μ, and AP-2σ was not significantly induced the change of sessile crystal cell population. In previous reports, mutation of *AP-2α* showed the similar phenotype of mutation of *Chc* (Windler and Bilder, 2010), suggesting the AP-2α plays a major role in the interaction with clathrin heavy chain. In summary, decrement of crystal cells caused by *abi* mutation is phenocopied by plasmatocyte-specific knockdown of WASp, Chc and AP-2α, or overexpression of dominant negative Cdc42, suggesting clathrin-mediated endocytosis acts in Abi-Cdc42-WASp pathway for regulating the crystal cell differentiation.

8.2. Macropinocytosis regulated by SCAR is not involved in crystal cell transdifferentiation.

Macropinocytosis is one type of clathrin-independent endocytosis which involves C-terminal Binding Protein1 (CtBP1) for the formation of macropinosome and Rabankyrin-5 for macropinosome maturation (Schnatwinkel et al., 2004; Haga et al., 2009; Saeed et al., 2010). Recent study in our lab has shown that Abi regulates BMP-dependent synaptic growth by macropinocytosis with Rac1-SCAR pathway (Kim et al., 2019). I next tested the influence of macropinocytosis on the crystal cell development in late stage. The Rho GTPase Rac is a key signaling mechanism for activating Arp2/3 complex-mediated actin polymerization. Compared with *eater-*

GAL4 control, plasmatocyte-specific overexpression of Rac1 dominant-negative form (Rac1-T17N) has no effect on sessile crystal cell population (Figure 23a and 23b). SCAR/WAVE complex is a downstream target of Rac1 serving the Arp2/3-dependent actin polymerization. Knockdown expression of SCAR in plasmatocytes did not make a significant difference compared to the control (Figure 23a and 23b). *Drosophila* has homologous proteins with CtBP1 and Rabankyrin-5, C-terminal Binding Protein (CtBP, CG7583) and Rabankyrin (CG41099; Fabrowski et al., 2013), respectively. Compared with *eater-GAL4* control, knockdown expression of either CtBP or Rabankyrin showed no significant change, statistically (Figure 23b). Taken together, plasmatocyte specific knockdown of SCAR, CtBP, and Rabankyrin or overexpression of dominant negative Rac1 has no effect on the crystal cell population. These results suggest that macropinocytosis with the Abi-Rac1-SCAR pathway might not be involved in the crystal cell development.

Figure 23. Impairment of Rac1-SCAR mediated macropinocytosis does not work on the process of the crystal cell differentiation.

(a) Images from posterior parts of late third instar larvae of *eater-GAL4/+* (Control, left), *eater-GAL4/UAS-Rac1T17N* ($Rac1^{T17N}$, middle) and *eater-GAL4/UAS-SCAR-RNAi* ($SCAR^{RNAi}$, right). Scale bar, 100 μm.

(b) The graph shows sessile crystal cell number of each genotype. Overexpression of dominant negative Rac1 or plasmatocyte-specific knockdown of *scar*, *ctbp,* and *rabankyrin* did not make a significant difference compared to control. 16 larvae were analyzed per each genotype.

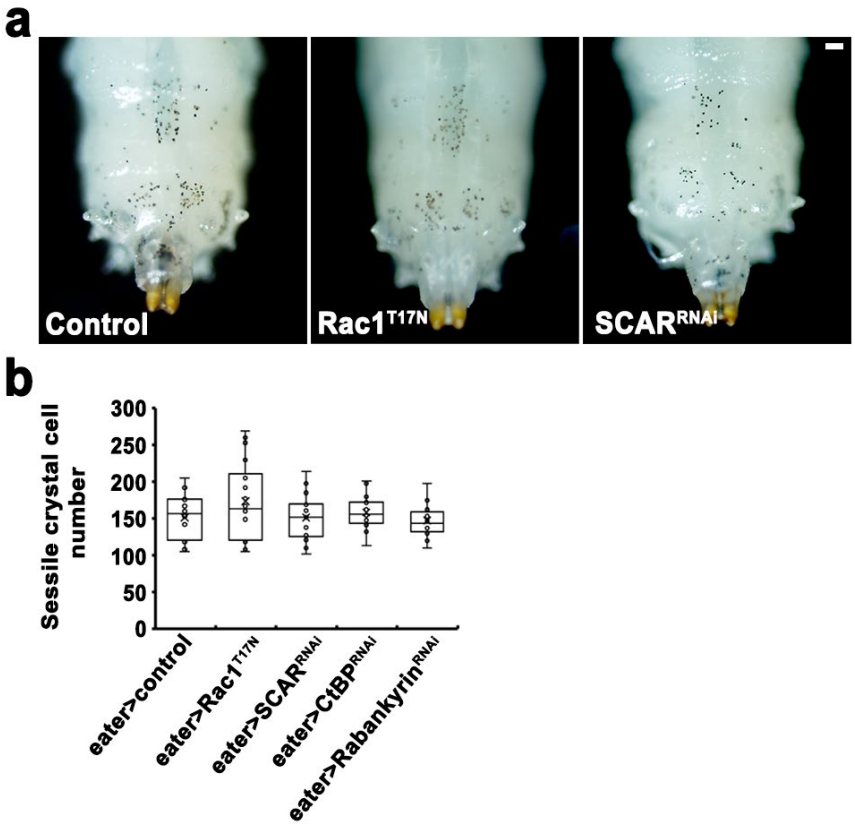
a
Control
Rac1T17N
SCARRNAi
b
Sessile crystal cell number
300
250
200
150
100
50
0
eater>control
eater>Rac1T17N
eater>SCARRNAi
eater>CtBPRNAi
eater>RabankyrinRNAi

8.3. Impairment of Graf-dependent GEEC does not affect crystal cell production.

The other type of clathrin-independent endocytosis is the GPI-enriched endocytic compartment (GEEC) endocytosis pathway. Sungdae Kim first demonstrated that *Drosophila* Graf is an essential component of the GEEC endocytosis in downregulating EGFR signaling and revealed a molecular mechanism underlying the recruitment of ubiquitylated cargoes to this clathrin-independent endocytic pathway (Kim et al., 2017). To verify whether the GEEC endocytosis affects the crystal cell differentiation in larval stages, *UAS-Graf-RNAi* was expressed with *eater-GAL4* drivers. Plasmatocyte-specific knockdown of Graf did not induce the decrement of sessile crystal cells (Figure 24a and 24b), suggesting that GEEC endocytosis does not influence the crystal cell differentiation in the late larval stage.

Figure 24. Loss of Graf does not influence the crystal cell differentiation.

(a) Images from posterior parts of late third instar larvae of *eater-GAL4/+* (Control, left) and *eater-GAL4/UAS-Graf-RNAi* ($Graf^{RNAi}$, right). Scale bar, 100 μm.

(b) The graph represents that plasmatocyte-specific knockdown of *graf* did not induce the decrement of sessile crystal cells. 16 larvae were analyzed per each genotype.

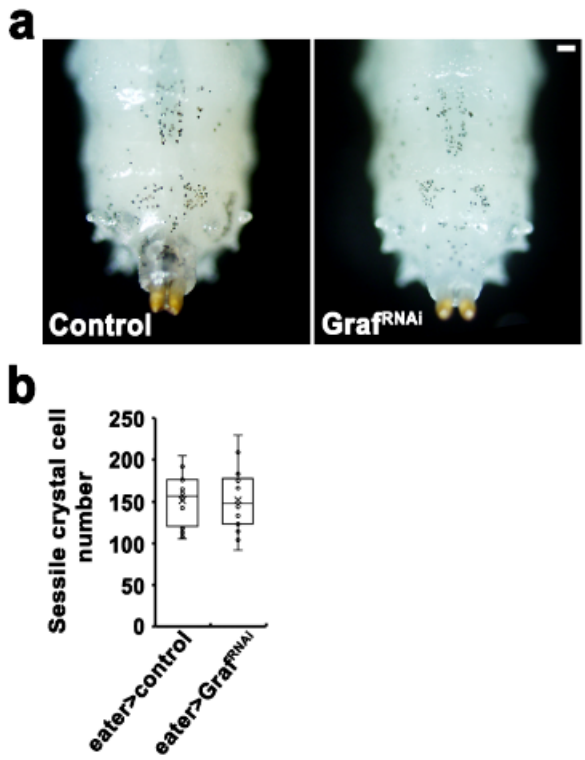
a
Control
Graf RNAi
b
Sessile crystal cell number
250
200
150
100
50
0
eater>control
eater>Graf RNAi

9. Serrate-induced Notch internalization is altered by the knockdown of *abi*.

9.1. Serrate-induced Notch internalization is blocked by the knockdown of *abi*.

The genetic data described above such as downregulation of Notch signaling in *abi* mutants and genetic interaction of *abi* with *notch* and *serrate* strongly support that Abi regulates Serrate mediated Notch signaling during transdifferentiation. In addition, the phenotypic similarities between the mutation of *abi*, *notch* and endocytic molecules suggest that endocytosis might be necessary for controlling Notch signaling by Abi. To unravel the function of Abi in Notch signaling at the cellular level, I set up the cell culture system for the exclusion of complexity within an organism to study of signaling mechanism (Klueg and Muskavitch, 1999). S2 cells, which derived from embryonic hemocytes, are suitable for this study. To try to mimic *in vivo* environment, co-culture system was adopted as a method.

The induced S2-Mt-N cells by copper sulfate were co-cultured with Myc-tagged Serrate-expressing cells to make the circumstance of ligand-dependent Notch signaling activation. Two hours after co-culture, internalized Notch receptors were localized in the endosomal structure with Serrate-positive vesicles in control cells (Figure 25, Control). This observation implicates that the localization of Notch receptor was dependent on the existence of their ligand. To find out the role of Abi that regulates Notch receptor endocytosis, I observed the changes of Notch localization

Figure 25. Serrate-induced Notch internalization is blocked by knockdown of *abi*, *Chc*, and *WASp*.

Confocal images of co-cultured S2-Mt-N cells labeled with anti-Necd antibody on surface (Surface Notch, first column, green) and in cytosol (Internal Notch, second column, red), and S2R+ cells transiently expressing Ser-Myc (third column, blue). The forth column for merged channels. In control, with the presence of Serrate, Notch receptor showed punctate form in cytoplasm colocalized with Serrate. Treatment of Notch expressing cells with *abi* dsRNA showed that Notch receptor was enriched at the adherent membrane with Serrate expressing cell, not observed in the cytoplasm. Treatment with *Chc* dsRNA in Notch expressing cells exhibited that Notch receptor internalization blocked as same as the phenotype of the treatment with *abi* dsRNA. In Notch expressing cells with *Rabankyrin* dsRNA displayed normal internalization of Notch receptor with Serrate. Notch receptor internalization is blocked by treatment with *WASp* dsRNA. Treatment with *SCAR* dsRNA in Notch expressing cells showed that Notch receptor was localized at the plasma membrane as well as in the cytoplasm. These results from a collaboration with Sungdae Kim in our laboratory (Seoul National University).

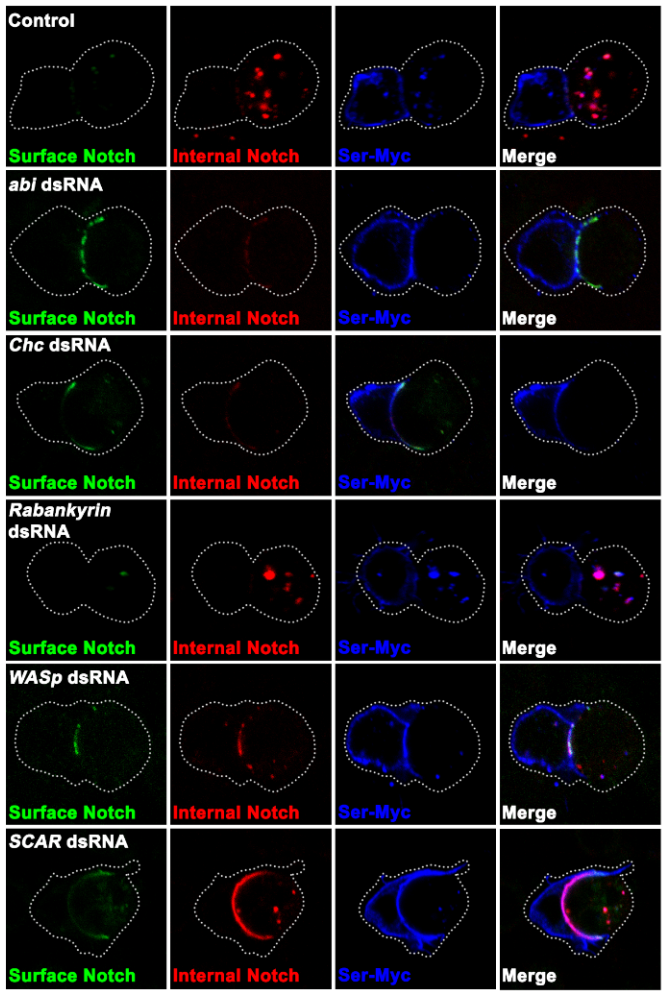
Control
Surface Notch
Internal Notch
Ser-Myc
Merge
abi dsRNA
Surface Notch
Internal Notch
Ser-Myc
Merge
Chc dsRNA
Surface Notch
Internal Notch
Ser-Myc
Merge
Rabankyrin dsRNA
Surface Notch
Internal Notch
Ser-Myc
Merge
WASp dsRNA
Surface Notch
Internal Notch
Ser-Myc
Merge
SCAR dsRNA
Surface Notch
Internal Notch
Ser-Myc
Merge

through the knockdown of *abi* in Notch expressing cells. First, I found that Notch expression itself was not affected by the knockdown of *abi* (Figure 25, *abi* dsRNA). Moreover, there was no problem in targeting the membrane that adhered to the Serrate expressing cells. However, Notch receptors are localized at the adherent membrane with Serrate expressing cell and could not be seen in the cytoplasm. These data support that Notch internalization is ligand-dependent and Serrate-induced Notch internalization is blocked by the knockdown of *abi*. Thus, Abi is a key molecule of Notch receptor endocytosis.

9.2. Abi-mediated Notch internalization is regulated by clathrin-dependent endocytosis.

The genetic data that I mentioned above strongly support the possibility that Abi-WASp complex might be involved in Notch signaling by clathrin-dependent endocytosis for sessile crystal cell population. The cellular data revealed that Abi is critical for the endocytosis of Notch receptors. To analyze which endocytic route is required for Notch internalization in the presence of Serrate, I examined the alteration of Notch receptor localization when each pathway component was knocked down by dsRNA.

Knockdown of *Chc* disrupted the internalization of Notch as shown in the knockdown of *abi* (Figure 25, *Chc* dsRNA). Treatment with *WASp* dsRNA also demonstrated the impairment of Notch internalization (Figure 25, *WASp* dsRNA). Knockdown of *SCAR* treated with dsRNA partially interrupted the Notch internalization

because the internalized Notch was detected in the cytoplasm (Figure 25, *SCAR* dsRNA). As expected, knockdown of *Rabankyrin* showed no complication in Notch internalization and the internalized Notch receptors were detected with Serrate-positive signals (Figure 25, *Rabankyrin* dsRNA). Collectively, Abi regulates Serrate-induced Notch endocytosis predominantly through clathrin-dependent pathway.

10. Abi functions in scab formation.

Loss-of-function mutations of *abi* induce the decrease of the crystal cell population in late larval stage, as previously described. Given that crystal cells function in wound healing and clotting, mature crystal cells can release prophenol oxidase required for melanization. Effectively, crystal cells are required to form a scab during wound healing (Galko et al., 2004; Neyen et al., 2015). When puncturing the surface of larvae with needle tip to make the wound artificially, melanized cells were observed and guided scab formation. I performed functional assays using this method to investigate whether melanization was affected by the reduction of crystal cells in the mutation of *abi*. In wild-type, all of the injured larvae formed scabs (Figure 26a and 26b). In addition, scabs formed immediately and required 40 minutes to produce melanized cells after puncture. However, scabs were observed in approximately 60% of abi^{5}/Df larvae and exhibited delays of 10 minutes after puncture (Figure 26a and 26b). These phenotypes are fully rescued by expression of Abi in plasmatocytes. Expressing Abi with the mutant form of WAB domain under the control of *eater-GAL4* driver had no influence on scab formation, though they were delays (Figure 26b, eater>$Abi^{\Delta 30-65}$ rescue). Thus, Abi-SCAR complex is not involved in the crystal cell function. Rescued larvae with plasmatocyte-specific expression of Abi mutant form in SH3 domain failed to form scabs with time delays after puncture (Figure 26b, eater>Abi^{W452K} rescue). Therefore, Abi mutants have

functional defects in the crystal cell activity, supporting that Abi–WASp pathway in transdifferentiation process has physiological significance in *Drosophila* hematopoietic system.

Figure 26. Loss of Abi delays melanization at the injury site.

(a) Live mount images after puncture wound assay in late third instar larvae of WT (upper panel) and *abi*^{5}/*Df* (lower panel). Yellow arrows indicate wound sites observing melanized scab. Anterior is left side. Scale bars, 50 μm.

(b) The graph displays the percentage of larvae with melanization at the wounded site. Larvae were analyzed at the indicated times after wounding. Note that all of injured wild-type larvae have melanized scab for 40 minutes post pricking. About 70% of wounded *abi*^{5}/*Df* larvae showed melanized scab for 60 minutes post pricking, with 10 minutes delay to form a scab. Larvae expressing Abi under the control of *eater-GAL4* driver (eater>Abi rescue) fully rescued the defect of scab formation. Larvae expressing Abi with the mutant form of WAB domain under the control of *eater-GAL4* driver (eater>Abi$^{\Delta 30-65}$ rescue) restored levels of scab formation compared to control. Larvae expressing Abi with the mutant in SH3 domain under the control of *eater-GAL4* driver (eater>Abi^{W452K} rescue) did not completely restore the failure of scab formation. 16 larvae were analyzed per each genotype. These results from a collaboration with Sungdae Kim in our laboratory (Seoul National University).

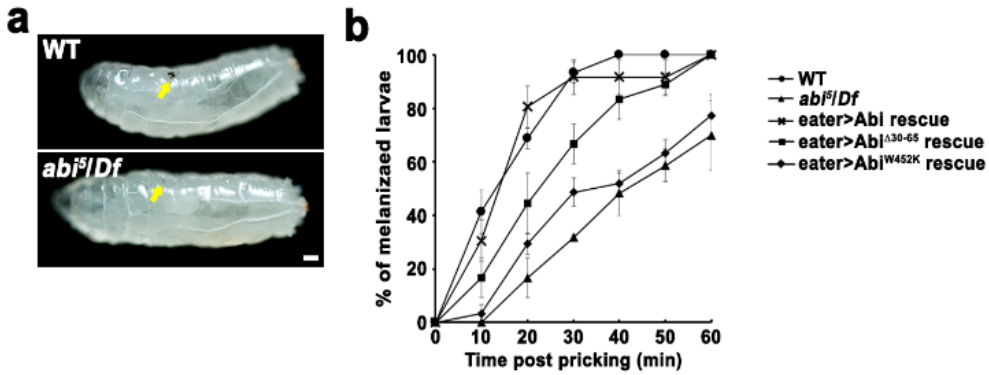
a
WT
abi5/Df
b
% of melanizaed larvae
Time post pricking (min)
0
20
40
60
80
100
0
10
20
30
40
50
60
WT
abi5/Df
eater>Abi rescue
eater>Abi Δ30-65 rescue
eater>Abi W452K rescue

Discussion

1. Abi functions in hemocyte differentiation during hematopoiesis

Research of the *Drosophila* hematopoietic system provides meaningful models studying the underlying components as fly hematopoiesis shares functions and mechanisms of evolutionarily conserved molecules with vertebrates. During fly development, each type of hemocytes undergoes proliferation and differentiation. Plasmatocytes, crystal cells, and lamellocytes are ultimately formed during *Drosophila* hematopoiesis. Three types of hemocytes are differentiated by specific signaling pathways dependent on the situation requiring their activity. Notch signaling is known to participate in the crystal cell specification and maintenance during embryogenesis. It has been known that the second step of the crystal cell development is controlled by Notch signaling occurring in larval stages. Moreover, Notch is necessary for massive differentiation of lamellocytes during infestation (Duvic et al., 2002). In mammals, Notch signaling regulates T cell development with stage-specific activation (Weng et al., 2004), and megakaryocyte differentiation (Mercher et al., 2008). However, the controlling mechanisms in the endocytic process of Notch signaling are poorly understood during crystal cell development.

Given my preceding data, *Drosophila* Abi as a regulator of hemocyte differentiation through endocytic modulation of Notch signaling in hematopoiesis. I discovered that the decrement of

crystal cells when the loss of Abi, only shown in late third instar stage with no changes in total hemocyte population. This phenotype was attributable to the defect in transdifferentiation from plasmatocytes to crystal cells accompanied by downregulation of Notch signaling. Genetic and cellular approaches implicated that alteration of Notch activity in *abi* mutants was caused by the blocking of Notch receptor internalization with impairment of clathrin-dependent endocytosis. Previous study reported that Notch could be internalized through clathrin-mediated endocytosis in fly eye disc (Windler and Bilder, 2010). With this research, I elicited that Clathrin-dependent pathway transduces Notch signaling in plasmatocyte transdifferentiation, and this pathway is mediated by Abi-WASp interaction. It is previously reported that Delta and Notch extracellular domain were colocalized with Sara-positive endosome at the mitotic stage during intestinal stem cell division (Montagne and Gonzalez-Gaitan, 2014). Further studies will reveal whether internalized Notch after Serrate binding goes through signaling endosome or not. Moreover, it should be determined whether the trafficking of Serrate and Notch requires Abi for targeting signaling endosomes.

The ability of wound healing is indispensable for the survival of organisms to endure the inhospitable environment. Wound healing is a response to injury of epithelial tissues or damage of fetal epidermis (Martin, 1997; Singer and Clark, 1999; Colwell et al., 2003). Melanization is an immune effector response to cuticle injury in the insect immune system. In *Drosophila*, wounding triggers the

rupture of mature circulating crystal cells and prophenoloxidase (PPO) release (Rizki et al., 1980; Gajewski et al., 2007). Crystal cells synthesize crystalline quantities of phenoloxidase (PO) that catalyze melanization. Larvae with mutation of *abi* have a functional defect in the crystal cell activity, and the rescue experiments support that interaction between Abi and WASp, not SCAR, is responsible for an efficient wound healing process of crystal cells. Thus, Abi-WASP pathway has physiological implication in the primary function of crystal cells.

2. The role of Abi in the regulation of signaling pathway through endocytosis

Endocytic molecules located in the endosomal compartment on these signaling pathways are known to be involved in hematopoiesis. Previous research studies have revealed that several signaling pathways play important roles in the process of hemocyte differentiation, such as Notch signaling (Duvic et al., 2002), EGFR signaling (Kim et al., 2017; Louradour et al., 2017), JAK/STAT pathway (Makki et al., 2010; Sinha et al., 2013) and so forth. Previous research in our lab reported that *Drosophila* Graf localizes prominently to early intermediates of the GEEC endocytic pathway and interacts directly with EGFR in a receptor ubiquitylation dependent manner to restrain plasmatocyte proliferation by inhibiting EGFR signaling (Kim et al., 2017). Rabex-5 negatively regulates Ras GTPase by promoting ubiquitylation of Ras, causing it to relocalize to an endosomal compartment, and act as a negative

regulator of Notch activity for appropriate proliferation and differentiation of hemocyte lineages (Reimels et al., 2015). Activated form of the ADP Ribosylation Factor 1 (ARF1) interacts with the hemocyte-specific endosomal protein Asrij to integrate multiple signalling pathways, including the JAK/STAT and Notch pathways as well as Pvr and Insulin signaling pathways, required to maintain blood cell homeostasis (Kulkarni et al., 2011; Khadilkar et al., 2017). Given these reports, it is indicated that endosomal regulation is an effective mechanism to coordinate signals in *Drosophila* hematopoiesis.

Drosophila Abi is previously reported to have endocytic functions in macropinocytosis (Figure 27, right side). Gbb-induced BMP receptor downregulation through macropinocytosis was encouraged by Abi with Abl-Rac-SCAR pathway to restrain synaptic growth. It has been known that Abi and SCAR/WAVE are crucial for Rac-dependent membrane protrusion and macropinocytosis. In addition, Abi also binds WASP through its C-terminal SH3 domain and stimulates WASP-dependent F-actin formation to regulate actin-based vesicular transport, endocytosis of epidermal growth factor receptor (EGFR), and surface distribution of EGFR and transferrin receptor (TfR) (Stephan et al., 2008). Thus, Abi is a dual regulator of WAVE and WASP activities in actin dynamics. According to my research, Abi is involved in clathrin-dependent endocytosis as well as macropinocytosis, indicating that it acts as a general endocytic adapter (Figure 27, left side).

Comparing the role of Abi that endocytoses BMP receptor in synaptic growth, this research found that Abi plays the same role as an endocytic molecule to internalize Notch receptor in hematopoiesis. Abi acts on the macropinocytosis to attenuate the BMP signaling, whereas it functions on the clathrin-mediated endocytosis to sustain the Notch signaling. In order to cooperate the discrete endocytic pathway, Abi interacts with distinct actin regulator, SCAR/WAVE for macropinocytosis and WASP for clathrin-dependent endocytosis. Because Abl-dependent phosphorylation enables Abi to bind the SCAR/WAVE complex, the dependency on Abl kinase is critical for changing the direction of Abi. It is believed that Abi and WASp are engaged in clathrin-dependent endocytosis while Abi-SCAR/WAVE pathway activated by Abl is associated with macropinocytosis. It is necessary to reveal the upstream signaling pathway that Abi determines the endocytic route depending on Abl role according to the cell context. The difference between clathrin-dependent endocytosis and macropinocytosis is not only the involvement of clathrin but the size of vesicles and morphological changes of the plasma membrane. Clathrin-coated pits on membrane invagination form vesicles of about 80-100 nm in diameter while macropinosomes follow membrane protrusion and exhibit over 200 nm in diameter (Kerr and Teasdale, 2009; McMahon and Boucrot, 2011). It can be fine-tuned that signal transduction is accompanied by the small size of endosomes such as clathrin-coated vesicles. But in the case of signaling hyperactivation, the cell needs an effective way to remove

large amounts of the receptor from the plasma membrane in order to prevent signaling. It would be more efficient to make vesicles with a large structure such as macropinosomes. Hence, a different range of actin dynamics is required for plasma membrane depending on the size of vesicles. Thereby, the unknown cue that determines the required amounts of actin filaments transmits its signal to Rho GTPases, resulting in the preference to WASP or SCAR/WAVE for actin polymerization.

As a consequence, these findings implicated that Abi regulates Notch signaling through clathrin-dependent pathway for transdifferentiation of plasmatocytes. Since the loss of human ABI is founded in primary myelofibrosis and acute myeloid leukemia, my research on identifying the physiological function of fly Abi will contribute to the understanding of the pathophysiological mechanism for associated human myeloproliferative neoplasms.

Figure 27. Current working model of Abi.

An illustration indicates Abi as a general endocytic adapter. It demonstrates the dual role of Abi. Left side represents that Abi acts on the sustentation of Notch signaling via WASP to clathrin-mediated internalize of Notch receptor in the crystal cell differentiation. Right side shows another role that the attenuation of BMP signaling through SCAR/WAVE to the macropinocytic uptake of BMP receptor in synaptic development.

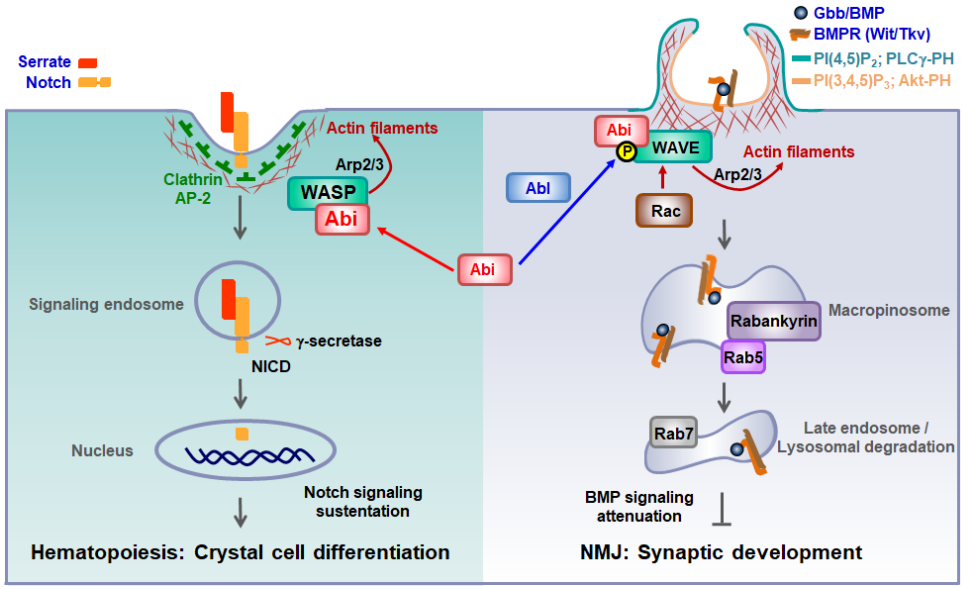
Gbb/BMP
BMPR (Wit/Tkv)
PI(4,5)P2; PLCγ-PH
PI(3,4,5)P3; Akt-PH
Serrate
Notch
Actin filaments
Arp2/3
Clathrin
AP-2
WASP
Abi
Abi
Abl
Abi
WAVE
P
Actin filaments
Arp2/3
Rac
Signaling endosome
γ-secretase
NICD
Rabankyrin
Macropinosome
Rab5
Nucleus
Rab7
Late endosome /
Lysosomal degradation
Notch signaling
sustentation
BMP signaling
attenuation
Hematopoiesis: Crystal cell differentiation
NMJ: Synaptic development

References

Banerjee U., Girard J.R., Goins L.M., and Spratford C.M. (2019) *Drosophila* as a Genetic Model for Hematopoiesis. Genetics 211, 367-417.

Barbui T., Thiele J., Gisslinger H., Kvasnicka H.M., Vannucchi A.M., Guglielmelli P., Orazi A., and Tefferi A. (2018) The 2016 WHO classification and diagnostic criteria for myeloproliferative neoplasms: document summary and in-depth discussion. Blood Cancer J 8, 15.

Bataillé, L., Auge, B., Ferjoux, G., Haenlin, M., and Waltzer, L. (2005). Resolving embryonic blood cell fate choice in *Drosophila*: interplay of GCM and RUNX factors. Development 132, 4635-4644.

Begum R., Nur-E-Kamal M.S., and Zaman M.A. (2004) The role of Rho GTPases in the regulation of the rearrangement of actin cytoskeleton and cell movement. Exp Mol Med 36, 358-66.

Bogdan S., Grewe O., Strunk M., Mertens A., and Klämbt C. (2004) Sra-1 interacts with Kette and Wasp and is required for neuronal and bristle development in *Drosophila*. Development 131, 3981-9.

Bogdan, S., Stephan, R., Lobke, C., Mertens, A., and Klambt, C. (2005). Abi activates WASP to promote sensory organ development. Nat Cell Biol 7, 977-984.

Bompard G. and Caron E. (2004). Regulation of WASP/WAVE proteins: making a long story short. J Cell Biol 166, 957-62.

Brand A.H. and Perrimon N. (1993) Targeted gene expression as a means of altering cell fates and generating dominant phenotypes. Development 118, 401-15.

Bretscher, A.J., Honti, V., Binggeli, O., Burri, O., Poidevin, M., Kurucz, E., Zsamboki, J., Ando, I., and Lemaitre, B. (2015). The Nimrod transmembrane receptor Eater is required for hemocyte

attachment to the sessile compartment in *Drosophila melanogaster*. Biol Open 4, 355-363.

Brückner, K., Kockel, L., Duchek, P., Luque, C.M., Rorth, P., and Perrimon, N. (2004). The PDGF/VEGF receptor controls blood cell survival in *Drosophila*. Dev Cell 7, 73-84.

Cantor A.B. and Orkin S.H. (2002) Transcriptional regulation of erythropoiesis: an affair involving multiple partners. Oncogene 21, 3368-76.

Chapman G., Major J.A., Iyer K., James A.C., Pursglove S.E., Moreau J.L., and Dunwoodie S.L. (2016) Notch1 endocytosis is induced by ligand and is required for signal transduction. Biochim Biophys Acta 1863, 166-77.

Chorzalska A., Morgan J., Ahsan N., Treaba D.O., Olszewski A.J., Petersen M., Kingston N., Cheng Y., Lombardo K., Schorl C., Yu X., Zini R., Pacilli A., Tepper A., Coburn J., Hryniewicz-Jankowska A., Zhao T.C., Oancea E., Reagan J.L., Liang O., Kotula L., Quesenberry P.J., Gruppuso P.A., Manfredini R., Vannucchi A.M., and Dubielecka P.M. (2018) Bone marrow-specific loss of ABI1 induces myeloproliferative neoplasm with features resembling human myelofibrosis. Blood 132, 2053-2066

Choudhury, S.D., Mushtaq, Z., Reddy-Alla, S., Balakrishnan, S.S., Thakur, R.S., Krishnan, K.S., Raghu, P., Ramaswami, M., and Kumar, V. (2016). sigma2-Adaptin Facilitates Basal Synaptic Transmission and Is Required for Regenerating Endo-Exo Cycling Pool Under High-Frequency Nerve Stimulation in *Drosophila*. Genetics 203, 369-385.

Colwell A.S., Longaker M.T., and Lorenz H.P. (2003) Fetal wound healing. Front Biosci 8, s1240-8.

Crozatier, M., Ubeda, J.M., Vincent, A., and Meister, M. (2004). Cellular immune response to parasitization in *Drosophila* requires the EBF orthologue collier. PLoS Biol 2, E196.

Daga A., Karlovich C.A., Dumstrei K., and Banerjee U. (1996) Patterning of cells in the *Drosophila* eye by Lozenge, which shares homologous domains with AML1. Genes Dev 10, 1194-205.

Dai Z. and Pendergast A.M. (1995) Abi-2, a novel SH3-containing protein interacts with the c-Abl tyrosine kinase and modulates c-Abl transforming activity. Genes Dev 9, 2569-82.

Dameshek W. (1951) Some speculations on the myeloproliferative syndromes. Blood 6, 372-5.

Doerks, T., Copley, R.R., Schultz, J., Ponting, C.P., and Bork, P. (2002). Systematic identification of novel protein domain families associated with nuclear functions. Genome Res 12, 47-56.

Dolezal, T., Dolezelova, E., Zurovec, M., and Bryant, P.J. (2005). A role for adenosine deaminase in *Drosophila* larval development. PLoS Biol 3, e201.

Döhner H., Weisdorf D.J., and Bloomfield C.D. (2015) Acute Myeloid Leukemia. N Engl J Med 373, 1136-52.

Dubielecka P.M., Cui P., Xiong X., Hossain S., Heck S., Angelov L., and Kotula L. (2010) Differential regulation of macropinocytosis by Abi1/Hssh3bp1 isoforms. PLoS One 5, e10430.

Duvic B., Hoffmann J.A., Meister M., and Royet J. (2002) Notch signaling controls lineage specification during *Drosophila* larval hematopoiesis. Curr Biol 12, 1923-7.

Echarri A., Lai M.J., Robinson M.R., and Pendergast A.M. (2004) Abl interactor 1 (Abi-1) wave-binding and SNARE domains regulate its nucleocytoplasmic shuttling, lamellipodium localization, and

wave-1 levels. Mol Cell Biol 24, 4979-93.

Evans C.J., Hartenstein V., and Banerjee U. (2003) Thicker than blood: conserved mechanisms in *Drosophila* and vertebrate hematopoiesis. Dev Cell 5, 673-90.

Evans J.M., Day J.P., Cabrero P., Dow J.A., and Davies S.A. (2008) A new role for a classical gene: white transports cyclic GMP. J Exp Biol 211, 890-9.

Evans, C.J., Liu, T., and Banerjee, U. (2014). *Drosophila* hematopoiesis: Markers and methods for molecular genetic analysis. Methods 68, 242-251.

Fabrowski P., Necakov A.S., Mumbauer S., Loeser E., Reversi A., Streichan S., Briggs J.A., and De Renzis S. (2013) Tubular endocytosis drives remodelling of the apical surface during epithelial morphogenesis in *Drosophila*. Nat Commun 4, 2244.

Fang, M., Li, J., Blauwkamp, T., Bhambhani, C., Campbell, N., and Cadigan, K.M. (2006). C-terminal-binding protein directly activates and represses Wnt transcriptional targets in *Drosophila*. EMBO J 25, 2735-2745.

Fujii M., Kawai K., Egami Y., and Araki N. (2013) Dissecting the roles of Rac1 activation and deactivation in macropinocytosis using microscopic photo-manipulation. Sci Rep 3, 2385.

Fujiwara, Y., Chang, A.N., Williams, A.M., and Orkin, S.H. (2004). Functional overlap of GATA-1 and GATA-2 in primitive hematopoietic development. Blood 103, 583-585.

Furriols M. and Bray S. (2001) A model Notch response element detects Suppressor of Hairless-dependent molecular switch. Curr Biol 11, 60-4.

Gajewski, K.M., Sorrentino, R.P., Lee, J.H., Zhang, Q., Russell, M., and

Schulz, R.A. (2007). Identification of a crystal cell-specific enhancer of the black cells prophenoloxidase gene in *Drosophila*. Genesis 45, 200-207.

Galko, M.J., and Krasnow, M.A. (2004). Cellular and genetic analysis of wound healing in *Drosophila* larvae. PLoS Biol 2, E239.

Haga, Y., Miwa, N., Jahangeer, S., Okada, T., and Nakamura, S. (2009). CtBP1/BARS is an activator of phospholipase D1 necessary for agonist-induced macropinocytosis. EMBO J 28, 1197-1207.

Hall A. (1998) Rho GTPases and the actin cytoskeleton. Science 279, 509-14.

Hirao N., Sato S., Gotoh T., Maruoka M., Suzuki J., Matsuda S., Shishido T., and Tani K. (2006) NESH (Abi-3) is present in the Abi/WAVE complex but does not promote c-Abl-mediated phosphorylation. FEBS Lett 580, 6464-70.

Honti, V., Csordas, G., Markus, R., Kurucz, E., Jankovics, F., and Ando, I. (2010) Cell lineage tracing reveals the plasticity of the hemocyte lineages and of the hematopoietic compartments in *Drosophila melanogaster*. Mol Immunol 47, 1997-2004.

Innocenti, M., Gerboth, S., Rottner, K., Lai, F.P., Hertzog, M., Stradal, T.E., Frittoli, E., Didry, D., Polo, S., and Disanza, A., (2005). Abi1 regulates the activity of N-WASP and WAVE in distinct actin-based processes. Nat Cell Biol 7, 969-976.

Jia D., Gomez T.S., Metlagel Z., Umetani J., Otwinowski Z., Rosen M.K., and Billadeau D.D. (2010) WASH and WAVE actin regulators of the Wiskott-Aldrich syndrome protein (WASP) family are controlled by analogous structurally related complexes. Proc Natl Acad Sci 107, 10442-7.

Jung, S.H., Evans, C.J., Uemura, C., and Banerjee, U. (2005). The

Drosophila lymph gland as a developmental model of hematopoiesis. Development 132, 2521-2533.

Kerr M.C. and Teasdale R.D. (2009) Defining macropinocytosis. Traffic 10, 364-71.

Khadilkar, R.J., Ray, A., Chetan, D.R., Sinha, A.R., Magadi, S.S., Kulkarni, V., and Inamdar, M.S. (2017). Differential modulation of the cellular and humoral immune responses in *Drosophila* is mediated by the endosomal ARF1-Asrij axis. Sci Rep 7, 118.

Kim, N., Kim, S., Nahm, M., Kopke, D., Kim, J., Cho, E., Lee M., Kim, S.H., Broadie, K., et al. (2019). BMP-dependent synaptic development requires Abi-Abl-Rac signaling of BMP receptor macropinocytosis. Nat Commun 10, 684.

Kim, S., Nahm, M., Kim, N., Kwon, Y., Kim, J., Choi, S., Choi, E.Y., Shim, J., Lee, C., and Lee, S. (2017). Graf regulates hematopoiesis through GEEC endocytosis of EGFR. Development 144, 4159-4172.

Klueg K.M. and Muskavitch M.A. (1999) Ligand-receptor interactions and trans-endocytosis of Delta, Serrate and Notch: members of the Notch signalling pathway in *Drosophila*. J Cell Sci 112, 3289-97.

Kotula L. (2012) Abi1, a critical molecule coordinating actin cytoskeleton reorganization with PI-3 kinase and growth signaling. FEBS Lett 586, 2790-4.

Kroeger, P.T. Jr., Shoue, D.A., Mezzacappa, F.M., Gerlach, G.F., Wingert, R.A., and Schulz, R.A. (2013). Knockdown of SCF(Skp2) function causes double-parked accumulation in the nucleus and DNA re-replication in *Drosophila* plasmatocytes. PLoS One 8, e79019.

Krzemien, J., Oyallon, J., Crozatier, M., and Vincent, A. (2010). Hematopoietic progenitors and hemocyte lineages in the *Drosophila* lymph gland. Dev Biol 346, 310-319.

Kulkarni, V., Khadilkar, R.J., Magadi, S.S., and Inamdar, M.S. (2011). Asrij maintains the stem cell niche and controls differentiation during *Drosophila* lymph gland hematopoiesis. PLoS One 6, e27667.

Kunda P., Craig G., Dominguez V., and Baum B. (2003) Abi, Sra1, and Kette control the stability and localization of SCAR/WAVE to regulate the formation of actin-based protrusions. Curr Biol 13, 1867-75.

Kurisu S. and Takenawa T. (2009) The WASP and WAVE family proteins. Genome Biol 10, 226.

Kurucz, E., Markus, R., Zsamboki, J., Folkl-Medzihradszky, K., Darula, Z., Vilmos, P., Udvardy, A., Krausz, I., Lukacsovich, T., Gateff, E., et al. (2007). Nimrod, a putative phagocytosis receptor with EGF repeats in *Drosophila* plasmatocytes. Curr Biol 17, 649-654.

Lanot, R., Zachary, D., Holder, F., and Meister, M. (2001). Postembryonic hematopoiesis in *Drosophila*. Dev Biol 230, 243-257.

Lebestky T., Chang T., Hartenstein V., and Banerjee U. (2000) Specification of *Drosophila* hematopoietic lineage by conserved transcription factors. Science 288, 146-9.

Lee, S., Nahm, M., Lee, M., Kwon, M., Kim, E., Zadeh, A.D., Cao, H., Kim, H.J., Lee, Z.H., Oh, S.B., et al. (2007). The F-actin-microtubule crosslinker Shot is a platform for Krasavietz-mediated translational regulation of midline axon repulsion. Development 134, 1767-1777.

Leitão, A.B., and Sucena, E. (2015). *Drosophila* sessile hemocyte clusters are true hematopoietic tissues that regulate larval blood cell differentiation. Elife 4.

Liebau, S., Steinestel, J., Linta, L., Kleger, A., Storch, A., Schoen, M., Steinestel, K., Proepper, C., Bockmann, J., Schmeisser, M.J., et al.

(2011). An SK3 channel/nWASP/Abi-1 complex is involved in early neurogenesis. PLoS One 6, e18148.

Ling, K.W., Ottersbach, K., van Hamburg, J.P., Oziemlak, A., Tsai, F.Y., Orkin, S.H., Ploemacher, R., Hendriks, R.W., and Dzierzak, E. (2004). GATA-2 plays two functionally distinct roles during the ontogeny of hematopoietic stem cells. J Exp Med 200, 871-882.

Loubéry S., Seum C., Moraleda A., Daeden A., Fürthauer M., and Gonzalez-Gaitan M. (2014) Uninflatable and Notch control the targeting of Sara endosomes during asymmetric division. Curr Biol 24, 2142-2148.

Louradour, I., Sharma, A., Morin-Poulard, I., Letourneau, M., Vincent, A., Crozatier, M., and Vanzo, N. (2017). Reactive oxygen species-dependent Toll/NF-κB activation in the *Drosophila* hematopoietic niche confers resistance to wasp parasitism. Elife 6.

Lowry, J.A., and Atchley, W.R. (2000). Molecular evolution of the GATA family of transcription factors: conservation within the DNA-binding domain. J Mol Evol 50, 103-115.

Maduro M.F. and Rothman J.H. (2002) Making worm guts: the gene regulatory network of the *Caenorhabditis elegans* endoderm. Dev Biol 246, 68-85.

Makhijani, K., Alexander, B., Tanaka, T., Rulifson, E., and Brückner, K. (2011). The peripheral nervous system supports blood cell homing and survival in the *Drosophila* larva. Development 138, 5379-5391.

Makki, R., Meister, M., Pennetier, D., Ubeda, J.M., Braun, A., Daburon, V., Krzemien, J., Bourbon, H.M., Zhou, R., Vincent, A., et al. (2010). A short receptor downregulates JAK/STAT signalling to control the *Drosophila* cellular immune response. PLoS Biol 8, e1000441.

Markus, R., Laurinyecz, B., Kurucz, E., Honti, V., Bajusz, I., Sipos, B., Somogyi, K., Kronhamn, J., Hultmark, D., and Ando, I. (2009). Sessile hemocytes as a hematopoietic compartment in *Drosophila melanogaster*. Proc Natl Acad Sci 106, 4805-4809.

Martin P. (1997) Wound healing —aiming for perfect skin regeneration. Science 276, 75-81.

McMahon H.T. and Boucrot E. (2011) Molecular mechanism and physiological functions of clathrin-mediated endocytosis. Nat Rev Mol Cell Biol 12, 517-33.

Meister, M. (2004). Blood cells of *Drosophila*: cell lineages and role in host defence. Current Opinion in Immunology 16, 10-15.

Mercher T., Cornejo M.G., Sears C., Kindler T., Moore S.A., Maillard I., Pear W.S., Aster J.C., and Gilliland D.G. (2008). Notch signaling specifies megakaryocyte development from hematopoietic stem cells. Cell Stem Cell. 3, 314-26.

Merrifield, C.J., Qualmann, B., Kessels, M.M., and Almers, W. (2004). Neural Wiskott Aldrich Syndrome Protein (N-WASP) and the Arp2/3 complex are recruited to sites of clathrin-mediated endocytosis in cultured fibroblasts. Eur J Cell Biol 83, 13-18.

Milchanowski, A.B., Henkenius, A.L., Narayanan, M., Hartenstein, V., and Banerjee, U. (2004). Identification and characterization of genes involved in embryonic crystal cell formation during *Drosophila* hematopoiesis. Genetics 168, 325-339.

Miyazaki K., Matsuda S., Ichigotani Y., Takenouchi Y., Hayashi K., Fukuda Y., Nimura Y., and Hamaguchi M. (2000) Isolation and characterization of a novel human gene (NESH) which encodes a putative signaling molecule similar to e3B1 protein. Biochim Biophys Acta 1493, 237-41.

Montagne, C., and Gonzalez-Gaitan, M. (2014). Sara endosomes and the asymmetric division of intestinal stem cells. Development 141, 2014-2023.

Mooren O.L., Galletta B.J., and Cooper J.A. (2012) Roles for actin assembly in endocytosis. Annu Rev Biochem 81, 661-86.

Nahm M., Kim S., Paik S.K., Lee S., Lee Z.H., Kim J., Lee D., Bae Y.C., and Lee S. (2010) dCIP4 (*Drosophila* Cdc42-interacting protein 4) restrains synaptic growth by inhibiting the secretion of the retrograde Glass bottom boat signal. J Neurosci 30, 8138-50.

Neyen, C., Bretscher, A.J., Binggeli, O., and Lemaitre, B. (2014). Methods to study *Drosophila* immunity. Methods 68, 116-128.

Neyen C., Binggeli O., Roversi P., Bertin L., Sleiman M.B., and Lemaitre B. (2015) The Black cells phenotype is caused by a point mutation in the *Drosophila* pro-phenoloxidase 1 gene that triggers melanization and hematopoietic defects. Dev Comp Immunol 50, 166-74.

Orkin S.H., Shivdasani R.A., Fujiwara Y., and McDevitt M.A. (1998) Transcription factor GATA-1 in megakaryocyte development. Stem Cells 16, 79-83.

Pai S.Y., Truitt M.L., Ting C.N., Leiden J.M., Glimcher L.H., and Ho I.C. (2003) Critical roles for transcription factor GATA-3 in thymocyte development. Immunity 19, 863-75.

Parolini O., Berardelli S., Riedl E., Bello-Fernandez C., Strobl H., Majdic O., and Knapp W. (1997) Expression of Wiskott-Aldrich syndrome protein (WASP) gene during hematopoietic differentiation. Blood 90, 70-5.

Petraki, S., Alexander, B., and Brückner, K. (2015). Assaying Blood Cell Populations of the *Drosophila melanogaster* Larva. J Vis Exp 105.

Price J.V., Savenye E.D., Lum D., and Breitkreutz A. (1997) Dominant enhancers of Egfr in *Drosophila melanogaster*: genetic links between the Notch and Egfr signaling pathways. Genetics 147, 1139-53.

Quintas-Cardama, A., and Cortes, J. (2009). Molecular biology of bcr-abl1-positive chronic myeloid leukemia. Blood 113, 1619-1630.

Rajak, P., Dutta, M., and Roy, S. (2015). Altered differential hemocyte count in 3rd instar larvae of *Drosophila melanogaster* as a response to chronic exposure of Acephate. Interdiscip Toxicol 8, 84-88.

Rappoport, J.Z., Taha, B.W., Lemeer, S., Benmerah, A., and Simon, S.M. (2003). The AP-2 complex is excluded from the dynamic population of plasma membrane-associated clathrin. J Biol Chem 278, 47357-47360.

Rehorn K.P., Thelen H., Michelson A.M., and Reuter R. (1996) A molecular aspect of hematopoiesis and endoderm development common to vertebrates and *Drosophila*. Development 122, 4023-31.

Reimels, T.A., and Pfleger, C.M. (2015). *Drosophila* Rabex-5 restricts Notch activity in hematopoietic cells and maintains hematopoietic homeostasis. J Cell Sci 128, 4512-4525.

Rizki T.M., Rizki R.M., and Grell E.H. (1980) A mutant affecting the crystal cells in *Drosophila melanogaster*. Wilehm Roux Arch Dev Biol 188, 91-99.

Rizki T.M. and Rizki R.M. (1992) Lamellocyte differentiation in *Drosophila* larvae parasitized by *Leptopilina*. Dev Comp Immunol 16, 103-10.

Rodrigues, N.P., Janzen, V., Forkert, R., Dombkowski, D.M., Boyd, A.S., Orkin, S.H., Enver, T., Vyas, P., and Scadden, D.T. (2005). Haploinsufficiency of GATA-2 perturbs adult hematopoietic

stem-cell homeostasis. Blood 106, 477-484.

Rottner K., Hänisch J., and Campellone K.G. (2010) WASH, WHAMM and JMY: regulation of Arp2/3 complex and beyond. Trends Cell Biol 20, 650-61.

Saeed, MF., Kolokoltsov, AA., Albrecht, T., and Davey, RA. (2010). Cellular entry of ebola virus involves uptake by a macropinocytosis-like mechanism and subsequent trafficking through early and late endosomes. PLoS Pathog 6, e1001110.

Sanchez-Sanchez, B.J., Urbano, J.M., Comber, K., Dragu, A., Wood, W., Stramer, B., and Martin-Bermudo, M.D. (2017). *Drosophila* Embryonic Hemocytes Produce Laminins to Strengthen Migratory Response. Cell Rep 21, 1461-1470.

Sato, M., Maruoka, M., and Takeya, T. (2012). Functional mechanisms and roles of adaptor proteins in abl-regulated cytoskeletal actin dynamics. J Signal Transduct 2012, 414913.

Schnatwinkel, C., Christoforidis, S., Lindsay, MR., Uttenweiler- Joseph, S., Wilm, M., Parton, RG., and Zerial, M. (2004). The Rab5 effector Rabankyrin-5 regulates and coordinates different endocytic mechanisms. PLoS Biol 2, E261.

Shi Y., Alin K., and Goff S.P. (1995) Abl-interactor-1, a novel SH3 protein binding to the carboxy-terminal portion of the Abl protein, suppresses v-abl transforming activity. Genes Dev 9, 2583-97.

Shibuya N., Taki T., Mugishima H., Chin M., Tsuchida M., Sako M., Kawa K., Ishii E., Miura I., Yanagisawa M., and Hayashi Y. (2001) t(10;11)-acute leukemias with MLL-AF10 and MLL-ABI1 chimeric transcripts: specific expression patterns of ABI1 gene in leukemia and solid tumor cell lines. Genes Chromosomes Cancer 32, 1-10.

Shivdasani R.A., Fujiwara Y., McDevitt M.A., and Orkin S.H. (1997) A lineage-selective knockout establishes the critical role of transcription factor GATA-1 in megakaryocyte growth and platelet development. EMBO J 16, 3965-73.

Singer A.J. and Clark R.A. (1999) Cutaneous wound healing. N Engl J Med 341, 738-46.

Singh, A., Winterbottom, E.F., Ji, Y.J., Hwang, Y.S., and Daar, I.O. (2013). Abelson interactor 1 (ABI1) and its interaction with Wiskott-Aldrich syndrome protein (wasp) are critical for proper eye formation in Xenopus embryos. J Biol Chem 288, 14135-14146.

Sinha, A., Khadilkar, R.J., S, V.K., Roychowdhury Sinha, A., and Inamdar, M.S. (2013). Conserved regulation of the Jak/STAT pathway by the endosomal protein asrij maintains stem cell potency. Cell Rep 4, 649-658.

So C.W., So C.K., Cheung N., Chew S.L., Sham M.H., and Chan L.C. (2000) The interaction between EEN and Abi-1, two MLL fusion partners, and synaptojanin and dynamin: implications for leukaemogenesis. Leukemia 14, 594-601.

Soderling S.H. (2009) Grab your partner with both hands: cytoskeletal remodeling by Arp2/3 signaling. Sci Signal 2, pe5.

Speck, N.A., and Gilliland, D.G. (2002). Core-binding factors in haematopoiesis and leukaemia. Nat Rev Cancer 2, 502-513.

Stephan R., Grevelhörster A., Wenderdel S., Klämbt C., and Bogdan S. (2008) Abi induces ectopic sensory organ formation by stimulating EGFR signaling. Mech Dev 125, 183-95.

Stofanko M., Kwon S.Y., and Badenhorst P. (2008) A misexpression screen to identify regulators of *Drosophila* larval hemocyte development. Genetics 180, 253-67.

Stradal T., Courtney K.D., Rottner K., Hahne P., Small J.V., and Pendergast A.M. (2001) The Abl interactor proteins localize to sites of actin polymerization at the tips of lamellipodia and filopodia. Curr Biol 11, 891-5.

Taki T., Shibuya N., Taniwaki M., Hanada R., Morishita K., Bessho F., Yanagisawa M., and Hayashi Y. (1998) ABI-1, a human homolog to mouse Abl-interactor 1, fuses the MLL gene in acute myeloid leukemia with t(10;11)(p11.2;q23). Blood 92, 1125-30.

Tani, K., Sato, S., Sukezane, T., Kojima, H., Hirose, H., Hanafusa, H., and Shishido, T. (2003). Abl interactor 1 promotes tyrosine 296 phosphorylation of mammalian enabled (Mena) by c-Abl kinase. J Biol Chem 278, 21685-21692.

Tepass U., Fessler L., Aziz A., and Hartenstein V. (1994) Embryonic origin of hemocytes and their relationship to cell death in *Drosophila*. Development 120, 1829-37.

Terriente-Felix, A., Li, J., Collins, S., Mulligan, A., Reekie, I., Bernard, F., Krejci, A., and Bray, S. (2013). Notch cooperates with Lozenge/Runx to lock haemocytes into a differentiation programme. Development 140, 926-937.

Tokusumi, T., Shoue, D.A., Tokusumi, Y., Stoller, J.R., and Schulz, R.A. (2009). New hemocyte-specific enhancer-reporter transgenes for the analysis of hematopoiesis in *Drosophila*. Genesis 47, 771-774.

Vardiman J.W., Thiele J., Arber D.A., Brunning R.D., Borowitz M.J., Porwit A., Harris N.L., Le Beau M.M., Hellström-Lindberg E., Tefferi A., and Bloomfield C.D. (2009) The 2008 revision of the World Health Organization (WHO) classification of myeloid neoplasms and acute leukemia: rationale and important changes. Blood 114, 937-51.

Waltzer L., Ferjoux G., Bataillé L., and Haenlin M. (2003) Cooperation between the GATA and RUNX factors Serpent and Lozenge during *Drosophila* hematopoiesis. EMBO J 22, 6516-25.

Weng A.P., Ferrando A.A., Lee W., Morris J.P.4th., Silverman L.B., Sanchez-Irizarry C., Blacklow S.C., Look A.T., Aster J.C. (2004) Activating mutations of NOTCH1 in human T cell acute lymphoblastic leukemia. Science. 306, 269–271.

Windler S.L. and Bilder D. (2010) Endocytic internalization routes required for delta/notch signaling. Curr Biol 20, 538-43.

Zacharioudaki, E., and Bray, S.J. (2014). Tools and methods for studying Notch signaling in *Drosophila melanogaster*. Methods 68, 173-182.

국문 초록

조혈과정에서 Abelson 상호작용 단백질인 Abi에 의한 Notch 신호전달의 조절

박 선 영

협동과정 뇌과학전공

서울대학교 대학원

Abi 단백질은 Abelson 상호작용 단백질로 명명되었으며, SCAR 복합체를 구성하는 요소로 small GTPase 중의 하나인 Rac1 신호전달을 Arp2/3 복합체로 전달하여 actin의 중합화를 촉진한다. 이전 연구에 따르면 Abi와 SCAR가 Rac에 의존하는 세포막 돌출과정과 macropinocytosis에 작용한다고 알려져 있다. Abi는 actin 중합화에 있어, SCAR 외에 WASp 단백질을 통해서도 이를 촉진한다고 알려졌으며, 이 때에는 Rac1이 아닌 Cdc42가 신호전달을 매개한다. 하지만 Cdc42-WASp 경로를 통한 Abi의 actin 조절이 가지는 생물학적 의미에 대해서는 규명된 바가 미미하다.

본 논문은 초파리의 Abi가 혈액세포 발생과정인 조혈과정에 미치는 영향에 대한 것이다. Abi 단백질은 혈액세포인 plasmatocyte와 crystal cell에서 발현하며, abi 돌연변이체 유충은 late third instar 단계에서 crystal cell의 수가 감소하고 Notch reporter인 NRE의 발현이 현저하게 줄어들어 있는 것을 발견하였다. 유전학적 연구를 통해 abi와

notch가 상호작용하여 crystal cell의 분화과정에 관여한다는 것을 확인하였으며, 이러한 결과들로 Abi가 Notch 신호전달을 조절하여 plasmatocyte에서 crystal cell로의 전환분화(transdifferentiation) 과정에 필수적으로 작용한다는 것을 증명하였다. 또한 Abi는 Notch 신호전달을 위해 Notch 수용체의 clathrin-dependent endocytosis를 촉진하는데 이 때에 Rac1-SCAR 신호전달보다는 Cdc42-WASp 신호전달을 활성화시켜서 actin을 조절한다는 것을 밝혔다. 따라서 본 연구는 초파리 모델을 이용하여 조혈과정에서 Abi의 생리적 기능을 규명한 것으로, 사람에서 Abi 단백질의 결손이 발견되는 골수증식성 종양의 병리학적 기전 연구에 활용될 수 있는 기초자료로서 충분한 가치가 있을 것으로 사료된다.

Keywords : Abi, Crystal cell, 전환분화, Notch 신호전달, Endocytosis, 조혈과정

Student Number : 2010-30122